

1
2
3
4
5
6
7
8
9
10
11
12
13
14
15
16
17
18
19
20
21
22
23
24
25
26
27
28
29
30
31
32
33
34
35
36
37
38
39
40
41
42
43
44
45
46
47
48
49
50
51
52
53
54
55

**DESIGN OF
AN INDUCTION PROBE
FOR SIMULTANEOUS MEASUREMENTS OF
PERMITTIVITY AND RESISTIVITY**

**PROGETTAZIONE DI
UNA SONDA AD INDUZIONE
PER MISURE SIMULATANEE DI
PERMITTIVITÀ E RESISITIVITÀ**

(Short Title - Titolo Abbreviato: RESPER *PROBE*)

Alessandro Settimi, Achille Zirizzotti, James A. Baskaradas, Cesidio Bianchi

*INGV (Istituto Nazionale di Geofisica e Vulcanologia) –
via di Vigna Murata 605, I-00143 Rome, Italy*

56
57
58
59
60
61
62
63
64
65
66
67
68
69
70
71
72
73
74
75
76
77
78
79
80
81
82
83
84
85
86
87
88
89
90
91
92
93
94
95
96
97
98
99
100
101
102
103
104
105
106
107
108
109
110
111
112
113
114
115
116

Index

117		
118		
119	Abstract.	5
120		
121	Introduction.	6
122		
123	Topic and structure of the paper.	6
124		
125	1. Mathcad simulations on non-saturated terrestrial ground and concretes.	8
126		
127	1.1. RESPER connected to uniform sampling ADCs.	9
128		
129	1.2. IQ sampling ADCs.	9
130		
131	1.3. Lock-in amplifiers.	11
132		
133	2. Characteristic geometrical dimensions of the RESPER probe.	13
134		
135	3. Conclusions.	15
136		
137	References.	17
138		
139	(Figures and captions)	(19)
140		
141		
142		
143		
144		
145		
146		
147		
148		
149		
150		
151		
152		
153		
154		
155		
156		
157		
158		
159		
160		
161		
162		
163		
164		
165		
166		
167		
168		

169
170
171
172
173
174
175
176
177
178
179
180
181
182
183
184
185
186
187
188
189
190
191
192
193
194
195
196
197
198
199
200
201
202
203
204
205
206
207
208
209
210
211
212
213
214
215
216
217
218
219

220
221
222
223
224
225
226
227
228
229
230
231
232
233
234
235
236
237
238
239
240
241
242
243
244
245
246
247
248
249
250
251
252
253
254
255
256
257
258
259
260
261
262
263
264
265
266
267
268
269
270
271
272
273
274
275

Abstract

In this paper, we propose a discussion of the theoretical design and move towards the development and engineering of an induction probe for electrical spectroscopy which performs simultaneous and non invasive measurements on the electrical RESistivity ρ and dielectric PERmittivity ϵ_r of non-saturated terrestrial ground and concretes (RESPER probe). In order to design a RESPER which measures ρ and ϵ_r with inaccuracies below a prefixed limit (10%) in a band of low frequencies (LF) ($B=100kHz$), the probe should be connected to an appropriate analogical digital converter (ADC), which samples in uniform or in phase and quadrature (IQ) mode, otherwise to a lock-in amplifier. The paper develops only a suitable number of numerical simulations, using Mathcad, which provide the working frequencies, the electrode-electrode distance and the optimization of the height above ground minimizing the inaccuracies of the RESPER, in galvanic or capacitive contact with terrestrial soils or concretes, of low or high resistivity. As findings of simulations, we underline that the performances of a lock-in amplifier are preferable even when compared to an IQ sampling ADC with high resolution, under the same operating conditions. As consequences in the practical applications: if the probe is connected to a data acquisition system (DAS) as an uniform or an IQ sampler, then it could be commercialized for companies of building and road paving, being employable for analyzing "in situ" only concretes; otherwise, if the DAS is a lock-in amplifier, the marketing would be for companies of geophysical prospecting, involved to analyze "in situ" even terrestrial soils.

Riassunto

In questo articolo, proponiamo una discussione del progetto teorico e ci muoviamo verso lo sviluppo e l'ingegnerizzazione di una sonda ad induzione per la spettroscopia elettrica che effettui misure simultanee e non invasive delle RESistività elettrica ρ e PERmittività dielettrica ϵ_r per suoli terrestri e calcestruzzi non saturi (sonda RESPER). Al fine di progettare un RESPER che misuri ρ e ϵ_r con incertezze al di sotto di un limite prefissato (10%) in una banda di basse frequenze (LF) ($B=100kHz$), la sonda dovrebbe essere connessa ad un convertitore analogico digitale (ADC) adeguato, che campioni in modo uniforme o in fase e quadratura (IQ), altrimenti ad un amplificatore *lock-in*. Il lavoro sviluppa esclusivamente un opportuno numero di simulazioni numeriche che, usando Mathcad, forniscono le frequenze di lavoro, la distanza elettrodo-elettrodo e l'ottimizzazione dell'altezza da terra che riducono al minimo le incertezze del RESPER, a contatto galvanico o capacitivo con suoli terrestri o calcestruzzi, di resistività bassa o alta. Come risultati delle simulazioni, teniamo a sottolineare che le prestazioni di un amplificatore *lock-in* sono preferibili anche ad un ADC a campionamento IQ con alta risoluzione di bit, sotto le stesse condizioni di funzionamento. Come conseguenze nelle applicazioni pratiche: se la sonda è connessa ad un sistema di acquisizione dati (DAS), come una campionatore uniforme o IQ, allora potrebbe essere commercializzata per le imprese di costruzione e di pavimentazione stradale, ed utilizzabile per l'analisi "in situ" solo dei calcestruzzi, altrimenti, se il DAS è un amplificatore *lock-in*, la commercializzazione sarebbe per le società di prospezione geofisica, interessate ad analizzare "in situ" anche i suoli terrestri.

276 **Introduction.**

277

278 Electrical resistivity and dielectric permittivity are two independent physical properties which
279 characterize the behavior of bodies when these are excited by an electromagnetic field. The measurements of
280 these properties provides crucial information regarding practical uses of bodies (for example, materials that
281 conduct electricity) and for countless other purposes.

282 We refer to [Grard, 1990, a-b][Grard and Tabbagh, 1991][Tabbagh et al.,1993], who have verified
283 experimentally that the complex permittivity (resistivity and dielectric constant) of ground can be measured
284 with a set of four electrodes carried on a vehicle. This new approach offers significant advantages over the
285 system first introduced by Wenner which gives only the resistivity and requires the manual insertion of the
286 four electrodes into the ground.

287 This technique allows for relatively high resistivity ranges where electromagnetic induction methods are not
288 applicable because the resistivity effect is too low and hidden by the magnetic susceptibility response. The
289 determination of the dielectric constant, which previously was exclusively based on high-frequency radar
290 techniques (above 30MHz), is now possible in a wide range of lower frequencies, which is extremely
291 important because this parameter is very sensitive to the presence of water.

292 Specially, we refer to [Vannaroni et al., 2004][Del Vento and Vannaroni, 2005]. The soil dielectric
293 spectroscopy probe (SDSP) determines the complex permittivity of the shallow subsoil from measurements
294 of the mutual impedance of a four-electrode system electrically coupled with the ground. The mutual
295 impedance is defined as the ratio of the voltage measured across a pair of receiving electrodes to the current
296 transmitted by a second pair of electrodes. The mutual impedance depends on the geometry of the electrode
297 array but also on the complex permittivity of the ground.

298 The measurements are performed in AC regime and the electrodes do not require low impedance DC
299 contacts with the soil. In fact, the terminals are capacitively coupled to the terrain and do not require any
300 galvanic contact. This feature presents two advantages. The first is that one can inject into the ground the
301 exciter current even in absence of effective electrodes-soil galvanic contact, making the system particularly
302 suitable to be hosted onboard a moving vehicle. The second relies on the fact that, in AC regime, one can
303 measure not only the conduction but also the displacements currents in the ground, thus obtaining
304 information on the polarizability of the substances contained in it.

305 The band of frequency is limited to the range 10kHz-1MHz. The lower limit is effectively imposed by
306 two facts: a) firstly, the Maxwell-Wagner effect which limits probe accuracy [Frolich, 1990], as the most
307 important limitation happens because of interface polarization effects that are stronger at low frequencies,
308 say below 1kHz depending of medium conductivity; b) secondly, the need to maintain the amplitude of the
309 current at measurable levels as, given the capacitive coupling between electrodes and soil, the current
310 magnitude is proportional to the frequency. On the other hand, the upper limit is suitably fixed to allow the
311 analysis of the system in a regime of quasi static approximation and neglect the velocity factor of the cables
312 used for the electrode harness, that in turn degrades the accuracy of the mutual impedance phase
313 measurements.

314

315 **Topic and structure of the paper.**

316

317 In the present paper, we propose a discussion of the theoretical design and move towards the
318 development and engineering of a induction probe for electrical spectroscopy which acquires complex
319 impedance in the field. By increasing the distance between the electrodes, it is possible to investigate the
320 electrical properties of sub-surface structures to greater depth. The probe can perform immediate
321 measurements on materials with high resistivity and permittivity, without subsequent stages of data analysis.
322 We refer to our previous papers [Settimi et al, 2009, a-b]. The first paper [Settimi et al, 2009, a] had
323 discussed the theoretical modelling of an induction probe which performs simultaneous and non invasive
324 measurements on the electrical RESistivity ρ and dielectric PERmittivity ϵ_r of non-saturated media (RESPER
325 probe). A mathematical-physical model was applied on propagation of errors in the measurement of
326 resistivity and permittivity based on the sensitivity functions tool [Murray-Smith, 1987]. The findings were
327 also compared to the results of the classical method of analysis in the frequency domain, which is useful for
328 determining the behaviour of zero and pole frequencies in the linear time invariant (LTI) circuit of the
329 quadrupole. The paper underlined that average values of electrical resistivity and dielectric permittivity may
330 be used to estimate the complex impedance over various terrains [Edwards, 1998] and concretes [Polder et
331 al., 2000][Laurents, 2005], especially when they are characterized by low levels of water content [Knight and

332 Nur, 1987] and analyzed within a bandwidth ranging only from LF to MF frequencies [Myounghak et al.,
333 2007][Al-Qadi et al., 1995]. In order to meet the design specifications which ensure satisfactory
334 performances of the probe (inaccuracy no more than 10%), the forecasts provided by the sensitivity functions
335 approach were discussed in comparison to those foreseen by the transfer functions method (in terms of both
336 the frequency f and measurable range of resistivity ρ or permittivity ϵ_r).

337 The second paper [Settimi et al, 2009, b] moves towards the practical implementation of electrical
338 spectroscopy. In order to design a RESPER which measures ρ and ϵ_r with inaccuracies below a prefixed limit
339 (10%) in a band of LF ($B=100kHz$), the probe should be connected to an appropriate analogical digital
340 converter (ADC), which samples in phase and quadrature (IQ) [Jankovic and Öhman, 2001] or in uniform
341 [Razavi, 1995] mode. If the probe is characterized by a galvanic contact with the surface, then the
342 inaccuracies in the measurement of resistivity and permittivity, due to the IQ or uniform sampling ADC, can
343 be analytically expressed. A large number of numerical simulations have proved that the performance of the
344 probe depends on the selected sampler and that the IQ is preferable when compared to the uniform mode
345 under the same operating conditions, i.e. number of bits and medium.

346 This paper develops only a suitable number of numerical simulations, using Mathcad, which provide
347 the working frequencies, the electrode-electrode distance and the optimization of the height above ground
348 minimizing the inaccuracies of the RESPER, in galvanic or capacitive contact with terrestrial soils or
349 concretes of low or high resistivity. As findings of simulations, we underline that the performances of a lock-
350 in amplifier [Scofield, 1994] are preferable even when compared to an IQ sampling ADC with high
351 resolution, under the same operating conditions. As consequences in the practical applications: if the probe is
352 connected to a DAS as an uniform or an IQ sampler, then it could be commercialized for companies of
353 building and road paving, being employable for analyzing “in situ” only concretes; otherwise, if the DAS is a
354 lock-in amplifier, the marketing would be for companies of geophysical prospecting, involved to analyze “in
355 situ” even terrestrial soils.

356 The paper is organized as follows. In section 1, Mathcad simulations on non-saturated terrestrial soils and
357 concretes are reported when the RESPER is connected to uniform (1.1) or IQ (1.2) sampling ADCs
358 otherwise to lock-in amplifiers (1.3). Sec. 2 deepens further the discussion on the design for the characteristic
359 geometrical dimensions of the probe. Conclusions are drawn in sec. 3.

360
361
362
363
364
365
366
367
368
369
370
371
372
373
374
375
376
377
378
379
380
381
382
383
384
385
386
387

388 1. Mathcad simulations on non-saturated terrestrial ground and concretes. 389

390 In this section, which refers to [Settimi et al, 2009, a-b], we propose to develop a suitable number of
391 simulations, using Mathcad, to design a RESPER, in galvanic or capacitive contact with a subjacent medium,
392 performing simultaneous and non invasive measurements for the electrical conductivity σ and the dielectric
393 permittivity ϵ_r . The RESPER is connected to a DAS, as an uniform / IQ sampling ADC or an lock-in
394 amplifier, which is appropriate for surfaces as the terrestrial ground or the concretes with high and low σ .
395 Deepening, the Mathcad simulations are applied to a quadrupolar probe [fig. 1], which interacts with the
396 medium by

- 397 • a galvanic contact or
- 398 • a capacitive contact,

399 the quadrupole being connected to a DAS [fig. 2], with specifications only similar to those of

- 400 1. one of the uniform sampling ADCs, NI-USB(or PCI, PXI)-51XX(or 61XX), with high speed or high
401 resolution or high density [Razavi, 1995], commercialized by the National Instruments Company, or
- 402 2. an IQ sampling ADC [Jankovic and Öhman, 2001], with high or low resolution, which are being
403 designed in our laboratories, or otherwise
- 404 3. one of lock-in amplifiers *SR810* and *SR830* [Scofield, 1994], commercialized by the Standford
405 Research Systems Company.

406 So, the simulations provide the ranges of measurability for the conductivity σ and the permittivity ϵ_r ,
407 describing various terrestrial soils and concretes, which minimize the inaccuracies in the measurements of
408 the probe, in galvanic contact, once designed its characteristic geometrical dimensions and selected its
409 frequency band, i.e. $B=100kHz$. Besides, the simulations provide the working frequencies, the electrode-
410 electrode distance and the optimization of the height above ground which minimize the inaccuracies of the
411 probe, in galvanic or capacitive contact with non-saturated terrestrial soils [Edwards, 1998], of high and low
412 conductivity, respectively as

413 A. flat, marshy, densely wooded in places ($\rho=1/\sigma=130\Omega\cdot m$, $\epsilon_r=13$) and

414 B. high-rise city centres, industrial areas ($\rho=3000\Omega\cdot m$, $\epsilon_r=4$),

415 or for concretes [Polder et al., 2000][Laurents et al., 2005] as (indoor climate carbonated) blast fumace slag,
416 fly ash cement and silica concrete fume, respectively with

417 C. high conductivity ($\rho=1/\sigma=4000\Omega\cdot m$, $\epsilon_r=9$) and

418 D. low conductivity ($\rho=10000\Omega\cdot m$, $\epsilon_r=4$).

419 Even if, according to Debye polarization mechanisms [Debye, 1929] or Cole-Cole diagrams [Auty and Cole,
420 1952], the complex permittivity of various materials in the frequency band from very low (VLF) to very high
421 (VHF) frequencies exhibits several intensive relaxation effects and a non-trivial dependence on the water
422 saturation [Chelidze and Gueguen, 1999][Chelidze et al., 1999], anyway average values of electrical
423 resistivity and dielectric permittivity may be used to estimate the complex impedance over various terrains
424 and concretes, especially when they are characterized by low levels of water content and analyzed within a
425 frequency bandwidth ranging only from LF to MF frequencies.

426
427 When $h=0$, i.e. the RESPER exhibits a galvanic contact with a subjacent medium characterized by an
428 electrical conductivity σ and a dielectric permittivity ϵ_r , the transfer impedance is a function of the working
429 frequency f such that its modulus $Z_N(f)$ is constant down to the cut-off frequency $f_T=f_T(\sigma,\epsilon_r)=\sigma/(2\pi\epsilon_0(\epsilon_r+1))$.
430 For a terrestrial ground of type A, $f_T=9.876MHz$; type B, $f_T=1.198MHz$; for concretes of type C, a lower
431 value $f_T=449.378kHz$, as the ratio σ/ϵ_r is lower in the concretes than in the terrestrial soils; type D close to
432 type C, $f_T=359.502kHz$, as σ/ϵ_r changes not so much in the concretes C and D. Only if the quadrupole probe
433 is in galvanic contact with the subjacent medium, i.e. $h=0$, then our mathematical-physical model predicts
434 that the inaccuracies $\Delta\sigma/\sigma(f)$ for σ and $\Delta\epsilon_r/\epsilon_r(f)$ for ϵ_r are invariant in the linear (Wenner's) or square
435 configuration and independent from the characteristic geometrical dimension of the quadrupole, i.e.
436 electrode-electrode distance L [Settimi et al., 2009, a].

437 When the quadrupole is in capacitive contact with the medium, an optimal ratio $x_{opt}=h_{pot}/L$ should be fixed
438 between the height h_{opt} above ground and L , in order to perform optimal measurements of the permittivity ϵ_r .
439 The square [fig. 3.a] configuration should be designed with an optimal height/dimension ratio $x_{opt,S}$ slightly
440 smaller than the corresponding linear (Wenner's) [fig. 3.b] ratio $x_{opt,W}$. In fact, for a terrestrial ground of type
441 A, $x_{opt,S}=0.046$ and $x_{opt,W}=0.052$; type B, $x_{opt,S}=0.078$ and $x_{opt,W}=0.087$; for concretes of type C, $x_{opt,S}=0.055$
442 and $x_{opt,W}=0.062$; type D identical to type B, $x_{opt,S}=0.078$ and $x_{opt,W}=0.087$, due to an equal permittivity $\epsilon_r=4$.
443 Then, both the configurations provide, in correspondence of the two ratio, i.e. $x_{opt,S}$ and $x_{opt,W}$, almost an

444 invariant position of the zero and pole frequencies for the transfer impedance in modulus, i.e. $z(x_{opt})$ and
 445 $p(x_{opt})$. Thus, for terrestrial soils of type A, $z_A=3.878MHz$ and $p_A=15.514MHz$; type B, $z_B=470.587kHz$ and
 446 $p_B=1.882MHz$; for concretes of type C, $z_C=176.47kHz$ and $p_C=705.881kHz$; type D, similar to type C,
 447 $z_D=141.176kHz$ and $p_D=564.705kHz$, as σ/ϵ_r is almost constant in the concretes C and D. Besides, chosen the
 448 DAS, both the configurations provide, in correspondence of the two ratio, i.e. $x_{opt,S}$ and $x_{opt,W}$, almost identical
 449 values for the inaccuracies in the measurements of σ and ϵ_r , i.e. $\Delta\sigma/\sigma(f)$ and $\Delta\epsilon_r/\epsilon_r(f)$ [Settimi et al, 2009, a].
 450

451 1.1. RESPER connected to uniform sampling ADCs.

452
 453 If the RESPER, of frequency band $B=100kHz$, has a galvanic contact with the subjacent medium, i.e.
 454 $h=0$, then, in order to measure the electrical conductivity σ and dielectric permittivity ϵ_r with inaccuracies,
 455 respectively $\Delta\sigma/\sigma$ and $\Delta\epsilon_r/\epsilon_r$, below a prefixed limit (10%), an uniform sampling ADC does not allow to
 456 perform measurements on terrestrial soils characterized by an high conductivity σ (type A) [fig. 4.a]. In fact,
 457 it is necessary $n_{min}=18$ [tab. 1.a] as minimal limit for the number of bits, too high to render the measuring
 458 system insensitive to the electrical noise of the external environment, as discussed in ref. (Settimi et al, 2009,
 459 b). Instead, the uniform sampling ADCs guarantee measurement of ϵ_r on terrestrial soils with a low σ (type
 460 B) [fig. 4.b]. In fact, it is sufficient to have $n_{min}=12$, even if the minimum value of working frequency f_{min} is
 461 too close to the end of the band B . In the best case, i.e. a high speed ADC only similar to the *NI PCI(PXI)-*
 462 *5124*, with sampling rate $f_S=200MHz$, it results $f_{min}=95.055kHz$, such that $\Delta\sigma/\sigma(f_{min})=2.4\cdot 10^{-3}$ [besides
 463 $f_{opt}=387.772kHz$, where $\Delta\sigma/\sigma(f_{opt})=8.825\cdot 10^{-3}$, $\Delta\epsilon_r/\epsilon_r(f_{opt})=0.017$] [tab. 1.b] [Settimi et al, 2009, b].
 464 Moreover, an uniform sampling ADC guarantees to perform measurements on concretes characterized by an
 465 high conductivity σ (type C) [fig. 4.c], with $n_{min}=12$ as minimal number of bits, though working in a small
 466 band $[f_{min}, B]$. In the best case, again a high speed ADC similar to the *NI PCI(PXI)-5124*, the minimum value
 467 of frequency is $f_{min}=33.315kHz$, such that $\Delta\sigma/\sigma(f_{min})=1.16\cdot 10^{-3}$ [besides $f_{opt}=193.94kHz$, where
 468 $\Delta\sigma/\sigma(f_{opt})=4.923\cdot 10^{-3}$, $\Delta\epsilon_r/\epsilon_r(f_{opt})=8.282\cdot 10^{-3}$] [tab. 1.c]. Instead, the uniform sampling ADCs guarantee
 469 measurements of ϵ_r on concretes with a low σ (type D) [fig. 4.d]. In fact, it is sufficient to have $n_{min}=8$, even
 470 if the minimum value of frequency f_{min} is too close to the end of the band B . In the best case, now a high
 471 speed ADC only similar to the *NI PCI(PXI)-5154*, with sampling rate $f_S=2GHz$, it results $f_{min}=94.953kHz$,
 472 such that $\Delta\sigma/\sigma(f_{min})=8.556\cdot 10^{-3}$ and $\Delta\epsilon_r/\epsilon_r(f_{min})=0.15$ [besides $f_{opt}=607.522kHz$, where $\Delta\sigma/\sigma(f_{opt})=0.033$,
 473 $\Delta\epsilon_r/\epsilon_r(f_{opt})=0.017$]. Then, it is necessary to have $n_{min}=12$ to work at least in a small band $[f_{min}, B]$. In the best
 474 case, again a high speed ADC similar to the *NI PCI(PXI)-5124*, it is $f_{min}=28.273kHz$, such that
 475 $\Delta\sigma/\sigma(f_{min})=1.059\cdot 10^{-3}$ [besides $f_{opt}=165.329kHz$, where $\Delta\sigma/\sigma(f_{opt})=4.346\cdot 10^{-3}$, $\Delta\epsilon_r/\epsilon_r(f_{opt})=8.19\cdot 10^{-3}$] [tab. 1.d]
 476 [Settimi et al, 2009, b]. In particular, an high density uniform ADC only similar to the *NI PCI-6110*, with
 477 number of bits $n=12$ and sampling rate $f_S=5MHz$, does not allow to perform measurements till $B=100kHz$:
 478 concerning the concretes characterized by an high conductivity σ (type C), only in the frequency band
 479 $[f_{min}=42.099kHz, f_{max}=95.531kHz]$, such that $\Delta\sigma/\sigma(f_{min})=0.034$ and $\Delta\sigma/\sigma(f_{max})=0.079$ [besides $f_{opt}=61.932kHz$,
 480 where $\Delta\sigma/\sigma(f_{opt})=0.051$, $\Delta\epsilon_r/\epsilon_r(f_{opt})=0.085$]; as regards the concretes with a low σ (type D), only in the band
 481 $[f_{min}=35.085kHz, f_{max}=85.396kHz]$, such that $\Delta\sigma/\sigma(f_{min})=0.029$ and $\Delta\sigma/\sigma(f_{max})=0.071$ [besides $f_{opt}=53.271kHz$,
 482 where $\Delta\sigma/\sigma(f_{opt})=0.044$, $\Delta\epsilon_r/\epsilon_r(f_{opt})=0.082$].
 483 Finally, a low cost ADC similar to the *NI USB-5133*, with $n=8$ and $f_S=100MHz$, guarantees measurements of
 484 ρ and ϵ_r which range from ($\rho_{min}=657.905\Omega\cdot m$, $\epsilon_{r,max}=81$) to ($\rho_{max}=20k\Omega\cdot m$, $\epsilon_{r,min}=2.31$), such that $\Delta\rho/\rho=0.013$,
 485 corresponding only to the unpolluted freshwater lakes with an electrical resistivity $\approx 1000\Omega\cdot m$ and a dielectric
 486 permittivity ≈ 80 [Edwards, 1998]. Instead, a low cost ADC similar to the *NI PCI(PXI)-5105*, with $n=12$ and
 487 $f_S=60MHz$ [fig. 5.a], guarantees measurements of ρ and ϵ_r which range from ($\rho_{min}=160.044\Omega\cdot m$, $\epsilon_{r,max}=81$),
 488 such that $\Delta\rho/\rho=7.181\cdot 10^{-3}$, to ($\rho_{max}=20k\Omega\cdot m$, $\epsilon_{r,min}=1$), such that $\Delta\rho/\rho=7.397\cdot 10^{-3}$ and $\Delta\epsilon_r/\epsilon_r=0.034$, so
 489 including also the arid sand deserts without vegetation with a resistivity $>20000\Omega\cdot m$ and a permittivity ≈ 3
 490 [Edwards, 1998], and especially various types of concretes across the types C to D.
 491

492 1.2. IQ sampling ADCs.

493
 494 If the RESPER, of frequency band $B=100kHz$, is in galvanic contact with the subjacent medium, i.e.
 495 $h=0$, then, in order to measure the electrical conductivity σ and the dielectric permittivity ϵ_r with inaccuracies
 496 below a prefixed limit (10%), the performances of an IQ sampling ADC are preferable when compared to an
 497 uniform sampling ADC. Under the same operating conditions, an uniform sampling can afford the advantage
 498 of the smallest resolution (i.e. $n=8$) to perform measurements on surfaces characterized by a low
 499 conductivity (i.e. the concretes), with the disadvantage to reduce the working band of frequency; in fact the

500 band B is higher than the maximum value of frequency f_{max} which allows an inaccuracy $\Delta\varepsilon_r/\varepsilon_r$ in the
 501 measurement of ε_r below the limit 10%. Instead, an IQ sampling can afford three advantages: first, over B ,
 502 the inaccuracies $\Delta\sigma/\sigma$ and $\Delta\varepsilon_r/\varepsilon_r$, respectively for σ and ε_r , are generally smaller by half an order of magnitude
 503 at least; second, the minimum value of frequency f_{min} which allows an inaccuracy $\Delta\varepsilon_r/\varepsilon_r(f)$ below 10% is
 504 generally slightly lower; third, the maximum value of frequency f_{max} is always higher than B ; as one and only
 505 disadvantage, using the IQ sampling, the optimal frequency f_{opt} which minimizes $\Delta\varepsilon_r/\varepsilon_r(f)$ is generally higher
 506 by half a decade of LF-MF frequency, at least, compared to the uniform sampling [Settimi et al, 2009, b].
 507 In fact, an IQ sampling guarantees to perform measurements on terrestrial soils characterized by an high
 508 conductivity σ (type A) [fig. 4.a], assuming necessarily $n_{min}=18$ [tab. 1.a] as minimal number of bits, too high
 509 to make the measuring system insensitive to the external electrical noise [Settimi et al, 2009, b]; and on
 510 terrestrial soils of low σ (type B) [fig. 4.b], with $n_{min}=12$, such that $f_{min}=94.228\text{kHz}$, where
 511 $\Delta\sigma/\sigma(f_{min})=9.819\cdot 10^{-4}$, being $B=100\text{kHz}$, where $\Delta\sigma/\sigma(B)=9.825\cdot 10^{-4}$ and $\Delta\varepsilon_r/\varepsilon_r(B)=0.089$ [besides
 512 $f_{opt}=1.459\text{MHz}$, where $\Delta\sigma/\sigma(f_{opt})=2.092\cdot 10^{-3}$, $\Delta\varepsilon_r/\varepsilon_r(f_{opt})=2.122\cdot 10^{-3}$] [tab. 1.b] [Settimi et al, 2009, b].
 513 Instead, the IQ sampling guarantees measurements on concretes with an high conductivity σ (type C) [fig.
 514 4.c], assuming $n_{min}=12$ as minimal number of bits, such that $f_{min}=33.292\text{kHz}$, where $\Delta\sigma/\sigma(f_{min})=9.813\cdot 10^{-4}$,
 515 being $\Delta\sigma/\sigma(B)=1.017\cdot 10^{-3}$ and $\Delta\varepsilon_r/\varepsilon_r(B)=0.012$ [besides $f_{opt}=547.144\text{kHz}$, where $\Delta\sigma/\sigma(f_{opt})=2.092\cdot 10^{-3}$,
 516 $\Delta\varepsilon_r/\varepsilon_r(f_{opt})=1.886\cdot 10^{-3}$] [tab. 1.c]; and on concretes of low σ (type D) [fig. 4.d], with $n_{min}=12$, so that
 517 $f_{min}=28.268\text{kHz}$, where $\Delta\sigma/\sigma(f_{min})=9.819\cdot 10^{-4}$, being $\Delta\sigma/\sigma(B)=1.039\cdot 10^{-3}$ and $\Delta\varepsilon_r/\varepsilon_r(B)=9.14\cdot 10^{-3}$ [besides
 518 $f_{opt}=437.637\text{kHz}$, where $\Delta\sigma/\sigma(f_{opt})=2.091\cdot 10^{-3}$, $\Delta\varepsilon_r/\varepsilon_r(f_{opt})=2.121\cdot 10^{-3}$] [tab. 1.d] [Settimi et al, 2009, b].
 519 Moreover, just in a laboratory which has an anechoic chamber, shielded from the external electrical noise,
 520 the quadrupolar probe can be connected to an uniform or IQ sampling ADC, characterized by an high
 521 resolution, in order to perform measurements on samples of various terrestrial soils, drawn from the outside
 522 environment [Settimi et al, 2009, b]. In fact, for both the uniform and IQ sampling, it is necessary to have
 523 $n_{min}=20$, as minimal number of bits, to measure, with inaccuracies below the limit of 10%, the electrical
 524 resistivity ρ and the dielectric permittivity ε_r which range from ($\rho_{min}=21.941\Omega\cdot m$, $\varepsilon_{r,max}=81$) to ($\rho_{max}=20\text{k}\Omega\cdot m$,
 525 $\varepsilon_{r,min}=1$), corresponding to various terrestrial soils included in the following list [Edwards, 1998]: pastoral,
 526 low hills, fertile soil ($\rho\approx 80\Omega\cdot m$, $\varepsilon_r\approx 15$); flat, marshy, densely wooded in places ($\approx 130\Omega\cdot m$, ≈ 13); pastoral,
 527 heavy clay soils, hills ($\approx 250\Omega\cdot m$, ≈ 12); pastoral, medium hills with forestation ($\approx 270\Omega\cdot m$, ≈ 12); rocky, sandy
 528 with some rainfall or some vegetation ($\approx 500\Omega\cdot m$, ≈ 8); rocky soil, steep forested hills, streams ($\approx 500\Omega\cdot m$,
 529 ≈ 10); low-rise city suburbs, built-up areas, parks ($\approx 1000\Omega\cdot m$, ≈ 6); high-rise city centres, industrial areas
 530 ($\approx 3000\Omega\cdot m$, ≈ 4). Then, it is necessary to have $n_{min}=24$ to measure, with inaccuracies below 10%, the
 531 resistivity ρ and the permittivity ε_r typical of agricultural plains, streams and rich loam soil ($\rho\approx 30\Omega\cdot m$,
 532 $\varepsilon_r\approx 20$). Finally, the above list does not include the sea water, away from river estuaries ($\approx 0.22\Omega\cdot m$, ≈ 81)
 533 [Edwards, 1998]. Instead, an IQ sampling, with number of bits $n=8$, guarantees measurements of ρ and ε_r
 534 ranging from ($\rho_{min}=674.098\Omega\cdot m$, $\varepsilon_{r,max}=81$) to ($\rho_{max}=20\text{k}\Omega\cdot m$, $\varepsilon_{r,min}=2.41$), where $\Delta\rho/\rho=0.017$, so, compared
 535 to the uniform sampling, a less wide variety of unpolluted freshwater lakes with a major inaccuracy in the
 536 measurements of the electrical resistivity and dielectric permittivity. Then, an IQ sampling, with $n=12$ [fig.
 537 5.b], guarantees measurements of ρ and ε_r ranging from ($\rho_{min}=154.937\Omega\cdot m$, $\varepsilon_{r,max}=81$), where $\Delta\rho/\rho=9.809\cdot 10^{-4}$,
 538 to ($\rho_{max}=20\text{k}\Omega\cdot m$, $\varepsilon_{r,min}=1$), where $\Delta\rho/\rho=1.017\cdot 10^{-3}$ and $\Delta\varepsilon_r/\varepsilon_r=0.022$, so, compared to the uniform
 539 sampling, even more arid sand deserts without vegetation with a minor inaccuracy for the resistivity and
 540 permittivity, and especially more types of concretes across the types C and D.
 541 Finally, when the quadrupole is in capacitive contact with the medium, being designed to perform optimal
 542 measurements, if an IQ sampling is used, then, almost independently from the probe configuration [Settimi
 543 et al, 2009, a], just the high resolution $n_{min}=18$ allows to measure the dielectric permittivity ε_r , with
 544 inaccuracy $\Delta\varepsilon_r/\varepsilon_r$, of terrestrial soils characterized by an high electrical conductivity σ (type A), with
 545 inaccuracy $\Delta\sigma/\sigma$ [fig. 4.a.bis]. The quadruple using the IQ sampling with $n_{min}=18$ could work in both MF at
 546 most one decade lower or better if within the band [$f_{up}=1.024\text{MHz}$, $z_A=3.878\text{MHz}$] and HF even three
 547 decades higher or better if within [$f_{low}=10.663\text{MHz}$, $p_A=15.514\text{MHz}$] [such that $\Delta\sigma/\sigma$ shows its minimum
 548 point in the upper limit f_{up} , so $\Delta\sigma/\sigma(f_{up})=2.527\cdot 10^{-5}$ and $\Delta\varepsilon_r/\varepsilon_r(f_{up})=3.028\cdot 10^{-4}$, while $\Delta\sigma/\sigma$ and $\Delta\varepsilon_r/\varepsilon_r$ are equal
 549 in the lower limit f_{low} , i.e. $\Delta\sigma/\sigma(f_{low})=\Delta\varepsilon_r/\varepsilon_r(f_{low})=3.194\cdot 10^{-5}$] [tab. 1.a.bis]. Instead, the minimal number of bits
 550 $n_{min}=12$ allows to measure the permittivity ε_r of: terrestrial soils with a low conductivity σ (type B) [fig.
 551 4.b.bis], for both MF at most half a decade lower than the band [$f_{up}=124.768\text{kHz}$, $z_B=470.587\text{kHz}$] and HF
 552 one decade higher than [$f_{low}=1.492\text{MHz}$, $p_B=1.882\text{MHz}$] [such that $\Delta\sigma/\sigma(f_{up})=1.64\cdot 10^{-3}$, $\Delta\varepsilon_r/\varepsilon_r(f_{up})=0.022$ and
 553 $\Delta\sigma/\sigma(f_{low})=\Delta\varepsilon_r/\varepsilon_r(f_{low})=2.311\cdot 10^{-3}$] [tab. 1.b.bis]; concretes with an high σ (type C) [fig. 4.c.bis], for both (MF
 554 at most about half a decade lower than) the band [$f_{up}=46.648\text{kHz}$, $z_C=176.47\text{kHz}$] and (HF about one decade
 555 higher than) [$f_{low}=499.469\text{kHz}$, $p_C=705.881\text{kHz}$] [such that $\Delta\sigma/\sigma(f_{up})=1.622\cdot 10^{-3}$, $\Delta\varepsilon_r/\varepsilon_r(f_{up})=0.02$ and

556 $\Delta\sigma/\sigma(f_{low})=\Delta\varepsilon_r/\varepsilon_r(f_{low})=2.092\cdot 10^{-3}$ [tab. 1.c.bis]; concretes with a low σ (type D) [fig. 4.d.bis], for both the
557 band $[f_{up}=37.43kHz, z_D=141.176kHz]$ and $[f_{low}=477.58kHz, p_D=564.705kHz]$ [such that $\Delta\sigma/\sigma(f_{up})=1.64\cdot 10^{-3}$,
558 $\Delta\varepsilon_r/\varepsilon_r(f_{up})=0.022$ and $\Delta\sigma/\sigma(f_{up})=\Delta\varepsilon_r/\varepsilon_r(f_{low})=2.311\cdot 10^{-3}$] [tab. 1.d.bis].
559

560 1.3. Lock-in amplifiers.

561
562 If the RESPER, of frequency band $B=100kHz$, is in galvanic contact with the subjacent medium, then,
563 in order to measure the electrical conductivity σ and the dielectric permittivity ε_r with inaccuracies below a
564 prefixed limit (10%), the performances of a lock-in amplifier only similar to the *SR810* (and *SR830*) are
565 preferable when compared to a IQ sampling ADC with number of bits $n_{IQ}=12$. In fact, the lock-in amplifier
566 is specified by a voltage sensitivity $\Delta V/V=2\cdot 10^{-9}$ and a degree phase resolution $\Delta\varphi=0.01^\circ$, so it guarantees
567 inaccuracies for the transfer impedance in modulus, i.e. $\Delta|Z|/|Z|_{lock-in}=2\cdot \Delta V/V=4\cdot 10^{-9}$, and in phase, i.e.
568 $\Delta\Phi/\Phi_{lock-in}=\Delta\varphi/360^\circ=2.778\cdot 10^{-5}$, that are smaller than the inaccuracies due to IQ sampling ADC
569 characterized by a number of bits $n_{IQ}=12$, respectively of five and one order of magnitude, i.e.
570 $\Delta|Z|/|Z|_{IQ}(n_{IQ})=\Delta\Phi/\Phi_{IQ,max}(n_{IQ})=1/2^{n_{IQ}}\approx 2.441\cdot 10^{-4}$ [Settimi et al, 2009, b]. Connecting the lock-in amplifier,
571 the inaccuracy $\Delta\varepsilon_r/\varepsilon_r(f)$ in the measurement of ε_r , as function of the frequency f , is like a concave upward
572 parabola which, compared to the IQ sampling ADC, shows a squashed shape around its minimum, being left
573 shifted towards LF and shifted downwards until smaller values. So, the lock-in amplifier, more than the IQ
574 sampling, guarantees: first, an optimal frequency f_{opt} , minimizing the inaccuracy $\Delta\varepsilon_r/\varepsilon_r(f)$ for ε_r , which is
575 lower of one MF decade, generally falling on middle frequencies (100kHz-1MHz) and, for almost all the
576 concretes, within the band $B=100kHz$; second, a minimal frequency f_{min} , allowing an inaccuracy $\Delta\varepsilon_r/\varepsilon_r(f)$
577 below the limit of 10%, which is smaller even of two LF decades, generally falling on low frequencies
578 ($\approx 1kHz$) and, for the concretes, on even lower frequencies ($\approx 100Hz$). Then, the inaccuracy $\Delta\varepsilon_r/\varepsilon_r(f)$ is
579 generally smaller by one magnitude order at least and three orders at most, while the inaccuracy $\Delta\sigma/\sigma(f)$ in
580 the measurement of σ can be approximated to a constant, i.e. $\Delta\sigma/\sigma\approx 2\cdot \Delta\Phi/\Phi_{lock-in}=5.556\cdot 10^{-5}$, since the
581 inaccuracy for $|Z|$, i.e. $\Delta|Z|/|Z|_{lock-in}=2\cdot \Delta V/V=4\cdot 10^{-9}$, is too little to contribute to the inaccuracy $\Delta\sigma/\sigma(f)$ of σ ,
582 so $\Delta\sigma/\sigma(f)=[1/S_{|Z|,\sigma}(f)]\cdot \Delta|Z|/|Z|_{lock-in}+ [1/S_{\Phi,\sigma}(f)]\cdot \Delta\Phi/\Phi_{lock-in}\approx [1/S_{\Phi,\sigma}(f)]\cdot \Delta\Phi/\Phi_{lock-in}$, and the sensitivity function
583 of Φ relative to σ , i.e. $S_{\Phi,\sigma}(f)\approx S_{\Phi,\sigma}(f)>=1/2$, is almost constant with the frequency f assuming the mean value
584 $1/2$, so $\Delta\sigma/\sigma(f)\approx 2\cdot \Delta\Phi/\Phi_{lock-in}$ [Settimi et al, 2009, a].

585 Differently from the IQ sampling ADC, with number of bits $n_{IQ}=12$, the lock-in amplifier guarantees to
586 perform measurements on terrestrial soils characterized by an high conductivity σ (type A) [fig. 4.a], so that
587 $f_{min}=2.9kHz$, where $\Delta\sigma/\sigma(f_{min})=5.556\cdot 10^{-5}$, being $B=100kHz$, where $\Delta\sigma/\sigma(B)=5.557\cdot 10^{-5}$ and
588 $\Delta\varepsilon_r/\varepsilon_r(B)=1.439\cdot 10^{-4}$ [besides $f_{opt}=1.199MHz$, where $\Delta\sigma/\sigma(f_{opt})=5.611\cdot 10^{-5}$, $\Delta\varepsilon_r/\varepsilon_r(f_{opt})=6.101\cdot 10^{-5}$] [tab. 1.a];
589 and on terrestrial soils of low σ (type B) [fig. 4.b], so that $f_{min}=379.08Hz$, where $\Delta\sigma/\sigma(f_{min})=5.556\cdot 10^{-5}$, being
590 $\Delta\sigma/\sigma(B)=5.582\cdot 10^{-5}$ and $\Delta\varepsilon_r/\varepsilon_r(B)=7.121\cdot 10^{-5}$ [besides $f_{opt}=145.489kHz$, where $\Delta\sigma/\sigma(f_{opt})=5.611\cdot 10^{-5}$,
591 $\Delta\varepsilon_r/\varepsilon_r(f_{opt})=7.081\cdot 10^{-5}$] [tab. 1.b]. In comparison to IQ sampling ADC, with $n_{IQ}=12$, the lock-in amplifier
592 guarantees more accurate measurements on concretes with an high conductivity σ (type C) [fig. 4.c], so that
593 $f_{min}=134.02Hz$, where $\Delta\sigma/\sigma(f_{min})=5.556\cdot 10^{-5}$, being $B=100kHz$, where $\Delta\sigma/\sigma(B)=5.738\cdot 10^{-5}$ and
594 $\Delta\varepsilon_r/\varepsilon_r(B)=6.393\cdot 10^{-5}$ [besides $f_{opt}=54.558kHz$, where $\Delta\sigma/\sigma(f_{opt})=5.611\cdot 10^{-5}$, $\Delta\varepsilon_r/\varepsilon_r(f_{opt})=6.295\cdot 10^{-5}$] [tab. 1.c];
595 and on concretes of low σ (type D) [fig. 4.d], so that $f_{min}=113.724Hz$, where $\Delta\sigma/\sigma(f_{min})=5.556\cdot 10^{-5}$, being
596 $\Delta\sigma/\sigma(B)=5.839\cdot 10^{-5}$ and $\Delta\varepsilon_r/\varepsilon_r(B)=7.311\cdot 10^{-5}$ [besides $f_{opt}=43.647kHz$, where $\Delta\sigma/\sigma(f_{opt})=5.611\cdot 10^{-5}$,
597 $\Delta\varepsilon_r/\varepsilon_r(f_{opt})=7.081\cdot 10^{-5}$] [tab. 1.d].

598 Moreover, if the quadrupolar probe is connected to a lock-in amplifier with specifications similar to the
599 *SR810*'s ones, then the measurements on various terrestrial soils can be performed extemporaneously and "in
600 situ", differently from connecting an IQ sampling ADC, characterized by an high bit resolution, when the
601 samples of those terrestrial soils must be drawn from the outside environment to be analyzed in a laboratory
602 which has an anechoic chamber, shielded from the external electrical noise [Settimi et al, 2009, b]. The lock-
603 in amplifier can not yet measure the resistivity ρ and the permittivity ε_r of the sea water, away from river
604 estuaries [Edwards, 1998], with inaccuracies $\Delta\rho/\rho$ and $\Delta\varepsilon_r/\varepsilon_r$ below 10%, but, in comparison to the IQ
605 sampling with a number of bit $n=24$, it can perform optimal measurements on even more conductive
606 agricultural plains, streams and richer loam soil [Edwards, 1998], though with inaccuracies generally higher
607 of two magnitude orders. In fact, the lock-in amplifier guarantees to measure ρ and ε_r ranging from
608 $(\rho_{min}=21.941\Omega\cdot m, \varepsilon_{r,max}=81)$, such that $\Delta\rho/\rho=5.557\cdot 10^{-5}$ and $\Delta\varepsilon_r/\varepsilon_r=1.371\cdot 10^{-4}$, to $(\rho_{max}=20k\Omega\cdot m, \varepsilon_{r,min}=1)$,
609 such that $\Delta\rho/\rho=5.738\cdot 10^{-5}$ and $\Delta\varepsilon_r/\varepsilon_r=1.151\cdot 10^{-4}$ [where $(\rho_{opt}=266.138\Omega\cdot m, \varepsilon_{r,opt}=81)$ such that
610 $\Delta\rho/\rho=5.611\cdot 10^{-5}$ and $\Delta\varepsilon_r/\varepsilon_r=5.735\cdot 10^{-5}$] [fig. 5.c]. Instead, an IQ sampling, with $n=24$, guarantees to measure
611 ρ and ε_r in the same range from $(\rho_{min}, \varepsilon_{r,max})$, such that $\Delta\rho/\rho=2.385\cdot 10^{-7}$ and $\Delta\varepsilon_r/\varepsilon_r=1.206\cdot 10^{-3}$, to $(\rho_{max}, \varepsilon_{r,min})$,

612 such that $\Delta\rho/\rho=2.483\cdot 10^{-7}$ and $\Delta\varepsilon_r/\varepsilon_r=5.302\cdot 10^{-6}$ [but where ($\rho_{opt}=2.669k\Omega\cdot m$, $\varepsilon_{r,opt}=81$) such that
613 $\Delta\rho/\rho=5.108\cdot 10^{-7}$ and $\Delta\varepsilon_r/\varepsilon_r=4.195\cdot 10^{-7}$].
614 Finally, if the quadrupole is in capacitive contact with the medium, being designed to perform optimal
615 measurements, then, almost independently from the probe configuration [Settimi et al, 2009, a], the
616 performances due to the lock-in amplifier are generally preferable when compared to an IQ sampling ADC
617 with high resolution [Settimi et al, 2009, b]. The upper limit f_{up} for the MF is only slightly left shifted
618 compared to an IQ sampling [being the upper limit f_{up} defined as the frequency where the inaccuracy $\Delta\sigma/\sigma(f)$
619 in the measurement of the electrical conductivity σ shows a point of minimum, i.e. $\partial_f\Delta\sigma/\sigma(f)|_{f=f_{up}}=0$]. The
620 lower limit f_{low} for the HF is right (types A-C) or left (type B-D) shifted compared to an IQ sampling [being
621 the lower limit f_{low} defined as the frequency where the inaccuracy $\Delta\sigma/\sigma(f)$ for the conductivity σ is equal to
622 the inaccuracy $\Delta\varepsilon_r/\varepsilon_r(f)$ for ε_r , i.e. $\Delta\sigma/\sigma(f_{low})=\Delta\varepsilon_r/\varepsilon_r(f_{low})$]. Numerically: type A, [$f_{up}=825.975kHz$,
623 $f_{low}=22.402MHz$] [tab. 1.a.bis]; type B, [$f_{up}=100.508kHz$, $f_{low}=780.277kHz$] [tab. 1.b.bis]; type C,
624 [$f_{up}=37.606kHz$, $f_{low}=546.487kHz$] [tab. 1.c.bis]; type D, [$f_{up}=30.152kHz$, $f_{low}=234.083kHz$] [tab. 1.d.bis].
625 Unfortunately, in the case of the terrestrial soils characterized by an high electrical conductivity σ (type A),
626 the inaccuracy $\Delta\varepsilon_r/\varepsilon_r(f)$, as function of the frequency f , is shifted upwards to values larger of almost one
627 magnitude order, due to an highest σ , so that the inaccuracy values increase of almost one order from 10^{-5}
628 until 10^{-4} . The band of the MF $f < f_{up}$ maintains almost invariant, a range of about one decade, as the HF band
629 $f > f_{low}$, a range of about three decades, compared to the IQ sampling with number of bits $n=18$. Numerically:
630 type A, $\Delta\sigma/\sigma(f_{up})=1.025\cdot 10^{-4}$, $\Delta\varepsilon_r/\varepsilon_r(f_{up})=8.192\cdot 10^{-4}$ and $\Delta\sigma/\sigma(f_{low})=\Delta\varepsilon_r/\varepsilon_r(f_{low})=1.925\cdot 10^{-4}$ [fig. 4.a.bis].
631 Rather, in the cases of terrestrial soils with a low conductivity σ (type B), concretes of high (type C) and low
632 (type D) σ , the inaccuracy $\Delta\varepsilon_r/\varepsilon_r(f)$, as function of the frequency f , is shifted downwards to values just higher
633 of one magnitude order and slightly towards lower frequencies, due to the effect of the lock-in amplifier, so
634 that the inaccuracy values decrease at least of one order from 10^{-3} until 10^{-4} . Even if the band of the MF $f < f_{up}$
635 is slightly broadened, anyway the HF band $f > f_{low}$ is broadened until two-three decades at most (type B-D) or
636 one decade at least (type C), compared to the IQ sampling of $n=12$. Numerically: type B, $\Delta\sigma/\sigma(f_{up})=1.041\cdot 10^{-4}$,
637 $\Delta\varepsilon_r/\varepsilon_r(f_{up})=9.487\cdot 10^{-4}$ and $\Delta\sigma/\sigma(f_{low})=\Delta\varepsilon_r/\varepsilon_r(f_{low})=1.037\cdot 10^{-4}$ [fig. 4.b.bis]; type C, $\Delta\sigma/\sigma(f_{up})=1.029\cdot 10^{-4}$,
638 $\Delta\varepsilon_r/\varepsilon_r(f_{up})=8.466\cdot 10^{-4}$ and $\Delta\sigma/\sigma(f_{low})=\Delta\varepsilon_r/\varepsilon_r(f_{low})=1.183\cdot 10^{-4}$ [fig. 4.c.bis]; type D, $\Delta\sigma/\sigma(f_{up})=1.041\cdot 10^{-4}$,
639 $\Delta\varepsilon_r/\varepsilon_r(f_{up})=9.478\cdot 10^{-4}$ and $\Delta\sigma/\sigma(f_{low})=\Delta\varepsilon_r/\varepsilon_r(f_{low})=1.037\cdot 10^{-4}$ [fig. 4.d.bis].
640
641
642
643
644
645
646
647
648
649
650
651
652
653
654
655
656
657
658
659
660
661
662
663
664
665
666
667

668 **2. Characteristic geometrical dimensions of the RESPER probe.**

669

670 In ref. [Settimi et al, 2009, b], we have demonstrated, once fixed the input resistance R_{in} of the
 671 amplifier stage and selected the working frequency f of the RESPER [fig. 1], which falls in a LF band
 672 starting from the minimum value of frequency f_{min} for operating conditions of galvanic contact or in a MF-
 673 HF band from the lower limit f_{low} for capacitive contact, that the minimal radius $r(R_{in}, f_{min})$ of the electrodes
 674 can be designed, as it depends only on the resistance R_{in} and the frequency f , being a function inversely
 675 proportional to both R_{in} and f ,

676
$$r \approx \frac{1}{(2\pi)^2 \varepsilon_0 R_{in} f} , \quad f \geq f_{min}, f_{low} . \quad (2.1)$$

677 Moreover, known the minimal number of bits n_{min} for the uniform or IQ sampling ADC [fig. 2], which
 678 allows an inaccuracy in the measurement of the dielectric permittivity ε_r below the prefixed limit 10%, also
 679 the electrode-electrode distance $L(r, n_{min})$ can be projected, as it depends only on the radius $r(R_{in}, f_{min})$ and the
 680 number of bits n_{min} , being directly proportional to $r(R_{in}, f_{min})$ and increasing as the exponential function $2^{n_{min}}$
 681 of n_{min} ,

682
$$L \propto r \cdot 2^{n_{min}} . \quad (2.2)$$

683 Finally, the radius $r(R_{in}, f_{min})$ maintains invariant whether the quadrupole probe assumes the square [fig. 3.a]
 684 or the linear (Wenner's) [fig. 3.b] configuration, while, known the number of bits n_{min} of the ADC, then the
 685 distance $L_S(r, n_{min})$ in the square configuration must be smaller of a factor $(2-2^{1/2})$ compared to the
 686 corresponding one $L_W(r, n_{min})$ in the Wenner's case,

687
$$L_S = (2 - \sqrt{2}) \cdot L_W = (2 - \sqrt{2}) \cdot r \cdot 2^{n_{min}} . \quad (2.3)$$

688 We suppose that the quadrupole is connected to an IQ sampling ADC, having engineered an electronic
 689 filter to remove the electrical noise of the external environment. In order to maintain the input resistance R_{in}
 690 of the amplifier stage around easily available values with magnitude order of $1-250M\Omega$ so below the almost
 691 impracticable limit of $1G\Omega$, the square configuration is preferable when compared to the linear (Wenner's)
 692 case [Settimi et al, 2009, a].

693 In fact, the square configuration, a part from the terrestrial ground characterized by an high electrical
 694 conductivity σ (type A), is fit for analyzing all the other surfaces, as the terrestrial soils with a low
 695 conductivity σ (type B) and the concretes of high (type C) or low (type D) σ , both in galvanic and in
 696 capacitive contact, though generally one should take the greatest care in designing the electrodes of this
 697 configuration, which require a non negligible radius around $417\mu m$, with the intent to reduce their
 698 interactions of capacitive coupling. Assume that the probe looks like a small electrical carpet designed to
 699 perform an electrical spectrography on road paving and buildings, i.e. a bi-dimensional array of characteristic
 700 geometrical dimension about $L \approx 1m$ both for terrestrial soils and concretes. With surfaces of type A, the
 701 probe is fit presenting only a capacitive contact, so that the amplifier stage should be projected with an input
 702 resistance $R_{in} = 41.19M\Omega$, while the electrodes with a radius $r \approx 6.514\mu m$, so, only in this case, without any
 703 interaction between the electrodes. Type B [fig. 6.a], the probe is fit presenting both a galvanic and a
 704 capacitive contact, so, in the first case, the amplifier must be projected with a resistance $R_{in} = 72.84M\Omega$, and
 705 the electrodes with a radius $r \approx 416.813\mu m$ [Settimi et al, 2009, b], while, in the second case, respectively
 706 $R_{in} = 4.6M\Omega$ and $r \approx 416.836\mu m$ [tab. 2.a]. Type C [fig. 6.b], in galvanic contact, the amplifier must be
 707 projected with a resistance $R_{in} = 206.1M\Omega$, and the electrodes with a radius $r \approx 416.94\mu m$, while, in capacitive
 708 contact, $R_{in} = 13.74M\Omega$ and $r \approx 416.866\mu m$ respectively [tab. 2.b]. Type D [fig. 6.c], in galvanic contact,
 709 $R_{in} = 242.8M\Omega$ and $r \approx 416.819\mu m$ [Settimi et al, 2009, b], while, in capacitive contact, $R_{in} = 14.37M\Omega$ and
 710 $r \approx 416.858\mu m$ respectively [tab. 2.c].

711 Instead, the Wenner's configuration, a part from the terrestrial ground characterized by a low electrical
 712 conductivity σ (type B), is fit for analyzing all the other surfaces, as the terrestrial soils with an high
 713 conductivity σ (type A) and the concretes of high (type C) or low (type D) σ , only in capacitive contact, with
 714 the advantage that generally the electrodes of this other configuration require a radius around $10-100\mu m$,
 715 small enough to avoid the occurrence of their capacitive coupling interactions. Assume that the probe is a
 716 coaxial cable designed for geophysical prospecting, i.e. a one-dimensional array of length $L_{tot} = 3L$ about
 717 $\approx 10m$, so only for terrestrial soils. With surfaces of type A, the probe is fit presenting only a capacitive
 718 contact, so that the amplifier stage should be projected with an input resistance $R_{in} = 21.09M\Omega$, while the
 719 electrodes with a radius $r \approx 12.721\mu m$. Type B [fig. 6.d], the probe is fit presenting both a galvanic and a
 720 capacitive contact, so, in the first case, the amplifier must be projected with a resistance $R_{in} = 37.3M\Omega$, and

721 the electrodes with a radius $r \approx 813.959 \mu m$ [Settimi et al, 2009, b], while, in the second case, $R_{in} = 2.356 M\Omega$
722 and $r = 813.856 \mu m$ respectively, so, compared to the previous cases, with an even stronger interaction
723 between the electrodes [tab. 2.d]. Finally, assume that the probe is a coaxial cable designed to perform an
724 electrical spectrography on buildings, i.e. a one-dimensional array of length about $L_{tot} \approx 1 m$, now only for the
725 concretes. Type C, only in capacitive contact, the amplifier must be projected with a resistance
726 $R_{in} = 70.38 M\Omega$, and the electrodes with a radius $r \approx 81.383 \mu m$. Type D, only in capacitive contact, $R_{in} = 73.6 M\Omega$
727 and $r \approx 81.389 \mu m$ respectively.
728
729
730
731
732
733
734
735
736
737
738
739
740
741
742
743
744
745
746
747
748
749
750
751
752
753
754
755
756
757
758
759
760
761
762
763
764
765
766
767
768
769
770
771
772
773
774
775
776

777 **3. Conclusions.**

778

779 The present paper has proposed a discussion of theoretical design and moved towards the development
780 and engineering of a induction probe for electrical spectroscopy which acquires complex impedance in the
781 field, filling the current technological gap.

782 Applying the same principle, but limited to the acquisition only of resistivity, there are various commercial
783 instruments used in geology for investigating the first 2-5 meters underground both for the exploration of
784 environmental areas and archaeological investigation [Samouëlian, 2005].

785 As regards the direct determination of the dielectric permittivity in subsoil, omitting geo-radar which
786 provides an estimate by complex measurement procedures on radar-gram processing [Declerk, 1995][Sbartai
787 et al., 2006], the only technical instrument currently used is the so-called time-domain reflectometer (TDR),
788 which utilizes two electrodes inserted deep in the ground in order to acquire this parameter for further
789 analysis [Mojid et al., 2003][Mojid and Cho, 2004].

790 Since, in our previous papers, we had already addressed and resolved the conceptual problem for
791 designing the “heart” of instrument, in this paper, we have completed the technical project [fig. 7] [tab. 3], in
792 forecast of the two next aims.

793 First aim: the implementation of an hardware which can handle many electrodes, arranged such as to
794 provide data which are related to various depths of investigation for a single pass of measurements; so, this
795 hardware must be able to switch automatically the transmitting and measurement couples.

796 The RESPER could be connected to a bi-dimensional array formed by a grid of coplanar electrodes, where a
797 multiplexer selects two transmitters and two receivers (geometrically similar to a small electrical *carpet* and
798 employable by a single operator with both hands). Through a series of 4×16 multiplexers, connected to the 4
799 inputs of probe, one selects different contacts of the electrical *carpet* in automatic way through an USB port.
800 In this way, shifting the position of measuring electrodes on the small *carpet*, there is possibility to obtain a
801 tomography without moving electrodes but simply by supporting the *carpet* and making to perform the
802 operations of selection and measurement by a program of control and processing.

803 Otherwise, the probe could be connected to an uni-dimensional array consisting of a simple coaxial cable
804 with antennas in line, where a muliplexer selects two transmitters and two receivers [only geometrically
805 similar to *Geometrics Ohmmapper* [Walker and Houser, 2002] and dragged on soils or by a single operator
806 or by a ground vehicle].

807 Second aim: the implementation of acquisition configurations, by an appropriate choice of the
808 transmission frequency, for the different applications in which this instrument can be profitably used.

809 If the RESPER is connected to a DAS as an uniform or rather an IQ sampling ADC, then it could be
810 commercialized for companies of building and road paving (ANAS), being employable for analyzing “in
811 situ” only concretes.

812 The probe, connected to a small electrical *carpet*, performs a scan, adhering on large areas, as cements with
813 high dielectric permittivity and draining asphalts. Then, the electrical *carpet*, being characterized by an area
814 of $1m^2$, tests only the most superficial part, usually up to about $1m$, in particular for measurements of
815 concretes. For manufactures of modern architecture and civil engineering, even if the small *carpet*
816 investigates properties which are not related directly with the mechanical resistance of concrete, anyway they
817 are related to its weaving, and therefore to its quality and actual state “in opera”. Moreover, the *carpet* allows
818 the quality check of asphaltting, especially when porous asphalts are placed to avoid the effect of
819 aquaplaning. This response lies mainly in dielectric permittivity, well known and constant for the mixture of
820 asphalt, but depending on its content in rubber and air.

821 If the RESPER is connected to a DAS as a lock-in amplifier, then it could be commercialized for companies
822 of geophysical prospecting, being employable for analyzing “in situ” even the terrestrial ground.

823 The probe, connected to a new instrument which could be named as *Ohm-Farad-Mapper (OFM)*, is lift off
824 ground, leading an electrical current through a system of antennas isolated from the terrestrial soil. Then, the
825 probe analyzes large stretches of land, using an *OFM*, of length about $10m$, with antennas in line which
826 provide a map of the soil, generally valid until the depth just of $10 m$. Moreover, the probe provides, as
827 regards pedological field, data on both the lithology of surface lands and on their water content at the time of
828 measurements, and, especially in view of that technological progress which names as precision agriculture,
829 data on the composition of both the land and fertilizers.

830 Finally, but certainly not last in terms of importance, the timing i.e. daily productivity in terms of
831 covered areas. The daily productivity in data acquisition is to be considered comparable with geo-radar,

832 which, as known, acquires the radar-gram while it is dragged, normally with a speed of one walking pace
833 (dozens of *cm/s* on manufactures, *1m* of profile per second on the surface of ground).

834
835
836
837
838
839
840
841
842
843
844
845
846
847
848
849
850
851
852
853
854
855
856
857
858
859
860
861
862
863
864
865
866
867
868
869
870
871
872
873
874
875
876
877
878
879
880
881
882
883
884
885
886
887

References.

- Al-Qadi I. L., Hazim O. A., Su W. and Riad S. M (1995): Dielectric properties of Portland cement concrete at low radio frequencies, *J. Mater. Civil. Eng.*, **7**, 192-198.
- Auty R.P. and Cole R.H. (1952): Dielectric properties of ice and solid, *J. Chem. Phys.*, **20**, 1309-1314.
- Chelidze T.L. and Gueguen Y. (1999): Electrical spectroscopy of porous rocks: a review-I, Theoretical models, *Geophys. J. Int.*, **137**, 1-15.
- Chelidze T.L., Gueguen Y. and Ruffet C. (1999): Electrical spectroscopy of porous rocks: a review-II, Experimental results and interpretation, *Geophys. J. Int.*, **137**, 16-34.
- Debye P. (1929): *Polar Molecules* (Leipzig Press, Germany).
- Declerk P. (1995): Bibliographic study of georadar principles, applications, advantages, and inconvenience, *NDT & E International*, **28**, 390-442 (in French, English abstract).
- Del Vento D. and Vannaroni G. (2005): Evaluation of a mutual impedance probe to search for water ice in the Martian shallow subsoil, *Rev. Sci. Instrum.*, **76**, 084504 (1-8).
- Edwards R. J. (1998): Typical Soil Characteristics of Various Terrains, <http://www.smeter.net/grounds/soil-electrical-resistance.php>.
- Frolich H. (1990): *Theory of Dielectrics* (Oxford University Press, Oxford).
- Grard R. (1990): A quadrupolar array for measuring the complex permittivity of the ground: application to earth prospection and planetary exploration, *Meas. Sci. Technol.*, **1**, 295-301.
- Grard R. (1990): A quadrupole system for measuring in situ the complex permittivity of materials: application to penetrators and landers for planetary exploration, *Meas. Sci. Technol.*, **1**, 801-806.
- Grard R. and Tabbagh A. (1991): A mobile four electrode array and its application to the electrical survey of planetary grounds at shallow depth, *J. Geophys. Res.*, **96**, 4117-4123.
- Jankovic D. and Öhman J. (2001): Extraction of in-phase and quadrature components by IF-sampling, Department of Signals and Systems, Cahlmers University of Technology, Goteborg (carried out at Ericson Microwave System AB).
- Knight R. J. and Nur A. (1987): The dielectric constant of sandstone, 60 kHz to 4 MHz, *Geophysics*, **52**, 644-654.
- Laurents S., Balayssac J. P., Rhazi J., Klysz G. and Arliguie G. (2005): Non-destructive evaluation of concrete moisture by GPR: experimental study and direct modeling, *Materials and Structures (M&S)*, **38**, 827-832 (2005).
- Mojid M. A., Wyseure G. C. L. and Rose D. A. (2003): Electrical conductivity problems associated with time-domain reflectometry (TDR) measurement in geotechnical engineering, *Geotechnical and Geological Engineering*, **21**, 243-258.
- Mojid M. A. and Cho H. (2004): Evaluation of the time-domain reflectometry (TDR)-measured composite dielectric constant of root-mixed soils for estimating soil-water content and root density, *J. Hydrol.*, **295**, 263-275.
- Murray-Smith D. J. (1987): Investigations of methods for the direct assessment of parameter sensitivity in linear closed-loop control systems, in *Complex and distributed systems: analysis, simulation and control*, edited by TZAFESTAS S. G. and BORNE P. (North-Holland, Amsterdam), pp. 323-328.
- Myounghak O., Yongsung K. and Junboum P. (2007): Factors affecting the complex permittivity spectrum of soil at a low frequency range of 1 kHz-10 MHz, *Environ Geol.*, **51**, 821-833.
- Polder R., Andrade C., Elsener B., Vennesland Ø., Gulikers J., Weidert R. and Raupach M. (2000): Test methods for on site measurements of resistivity of concretes, *Materials and Structures (M&S)*, **33**, 603-611.
- Razavi B. (1995): *Principles of Data Conversion System Design* (IEEE Press).
- Samouëlian A., Cousin I., Tabbagh A., Bruand A. and Richard G. (2005): Electrical resistivity survey in soil science: a review, *Soil Till. Res.* **83** 172-193.
- Sbartai Z. M., Laurents S., Balayssac J. P., Arliguie G. and Ballivy G. (2006): Ability of the direct wave of radar ground-coupled antenna for NDT of concrete structures, *NDT & E International*, **39**, 400-407.
- Scofield J. H. (1994): A Frequency-Domain Description of a Lock-in Amplifier, *American Journal of Physics (AJP)*, **62**, 129-133.
- Settimi A., Zirizzotti A., Baskaradas J. A. and Bianchi C. (2010): Inaccuracy assessment for simultaneous measurements of resistivity and permittivity applying a sensitivity and transfer function approaches, in press on *Ann. Geophys.- Italy (Earth-Prints)*, <http://hdl.handle.net/2122/5180>.

- Settimi A., Zirizzotti A., Baskaradas J. A. and Bianchi C. (2009): Optimal requirements of a data acquisition system for a quadrupolar probe employed in electrical spectroscopy (Earth-Prints, <http://hdl.handle.net/2122/5176>).
- Tabbagh A., Hesse A. And Grard R. (1993): Determination of electrical properties of the ground at shallow depth with an electrostatic quadrupole: field trials on archaeological sites, *Geophys. Prospect.*, **41**, 579-597.
- Vannaroni G., Pettinelli E., Ottonello C., Cereti A., Della Monica G., Del Vento D., Di Lellis A. M., Di Maio R., Filippini R., Galli A., Menghini A., Orosei R., Orsini S., Pagnan S., Paolucci F., Pisani A. R., Schettini G., Storini M. and Tacconi G. (2004): MUSES: multi-sensor soil electromagnetic sounding, *Planet. Space Sci.*, **52**, 67–78.
- Walker J. P. and Houser P. R. (2002): Evaluation of the OhmMapper instrument for soil moisture measurement, *Soil Science Society of America Journal*, **66**, 728-734 (<http://www.geometrics.com/geometrics-products/geometrics-electro-magnetic-products/ohm-mapper/>).

Figures and captions.

Figure 1

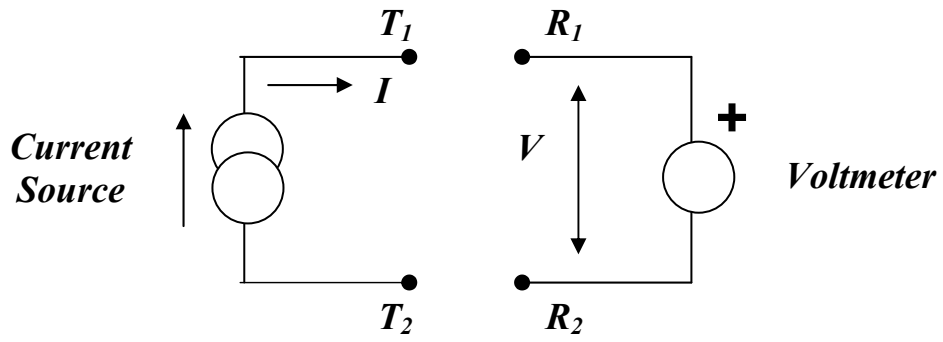


Figure 2

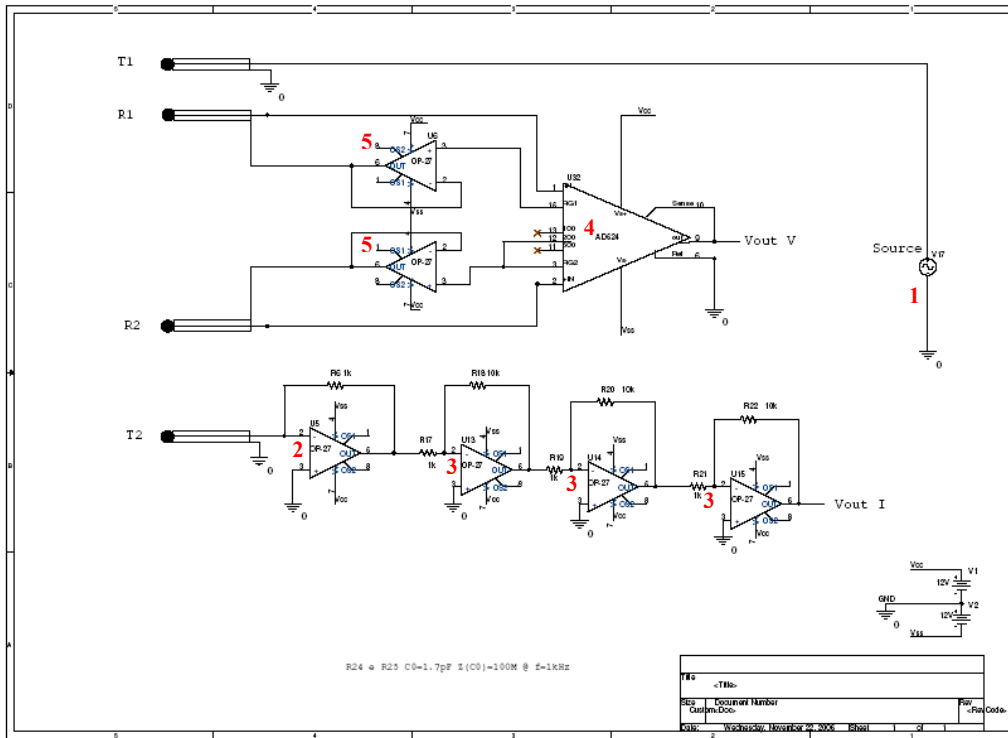
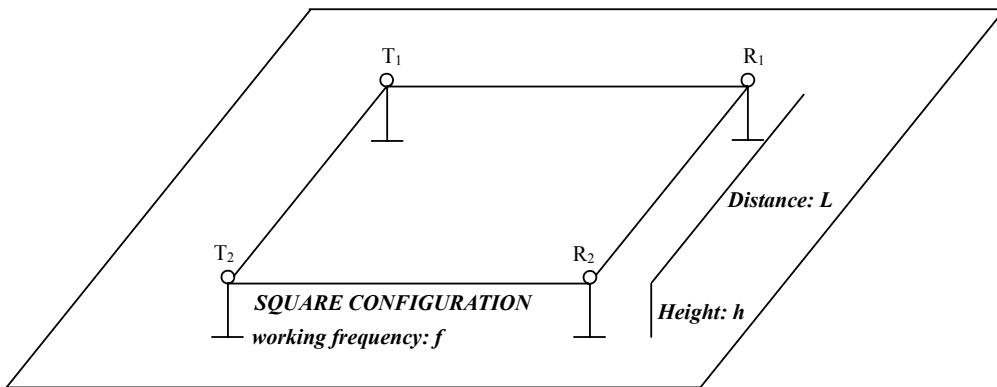


Figure 3.a

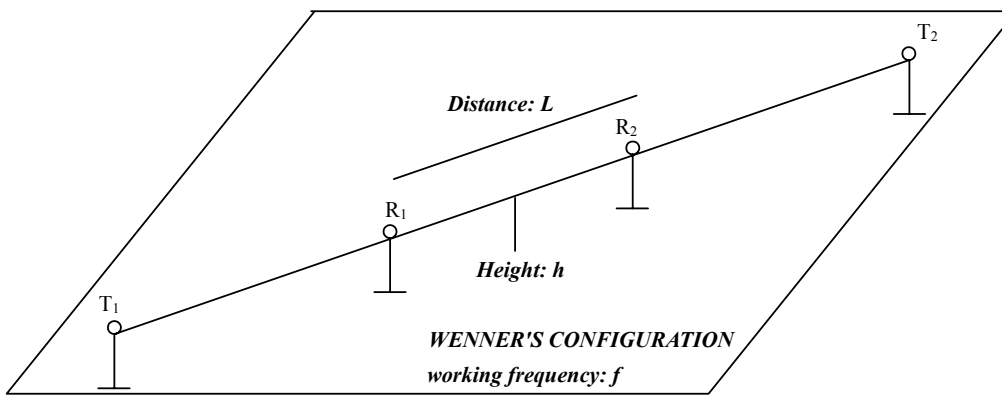


SUBSURFACE

Electrical Conductivity: σ

Dielectric Permittivity: ϵ_r

Figure 3.b



SUBSURFACE

Electrical Conductivity: σ

Dielectric Permittivity: ϵ_r

Figure. 4.a

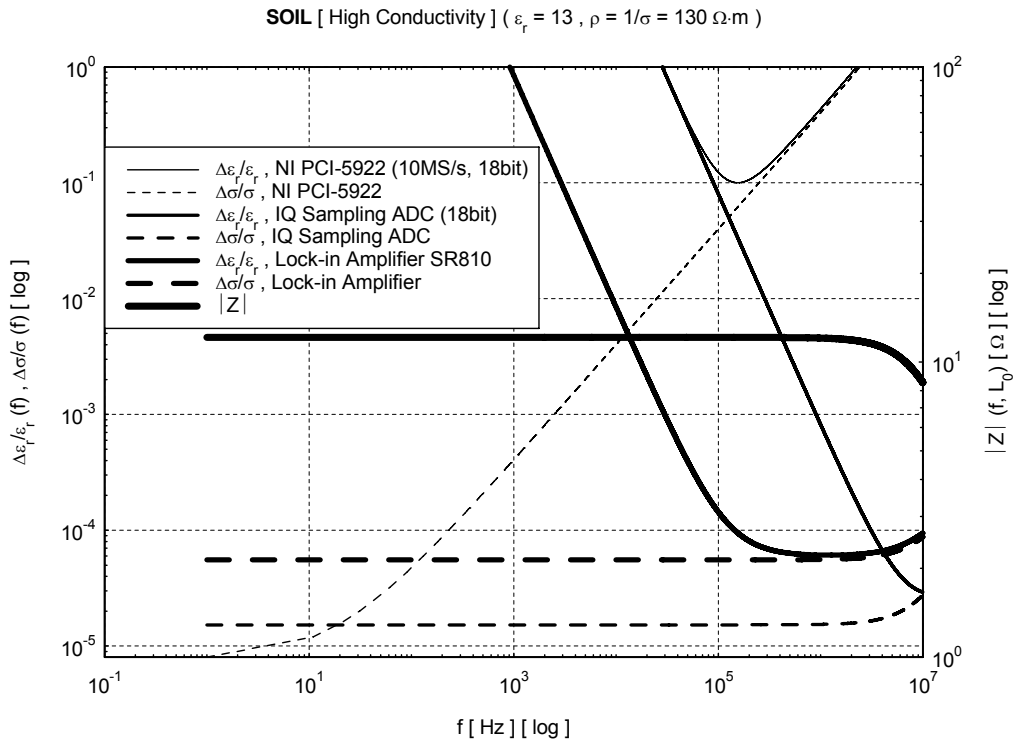


Figure 4.a.bis

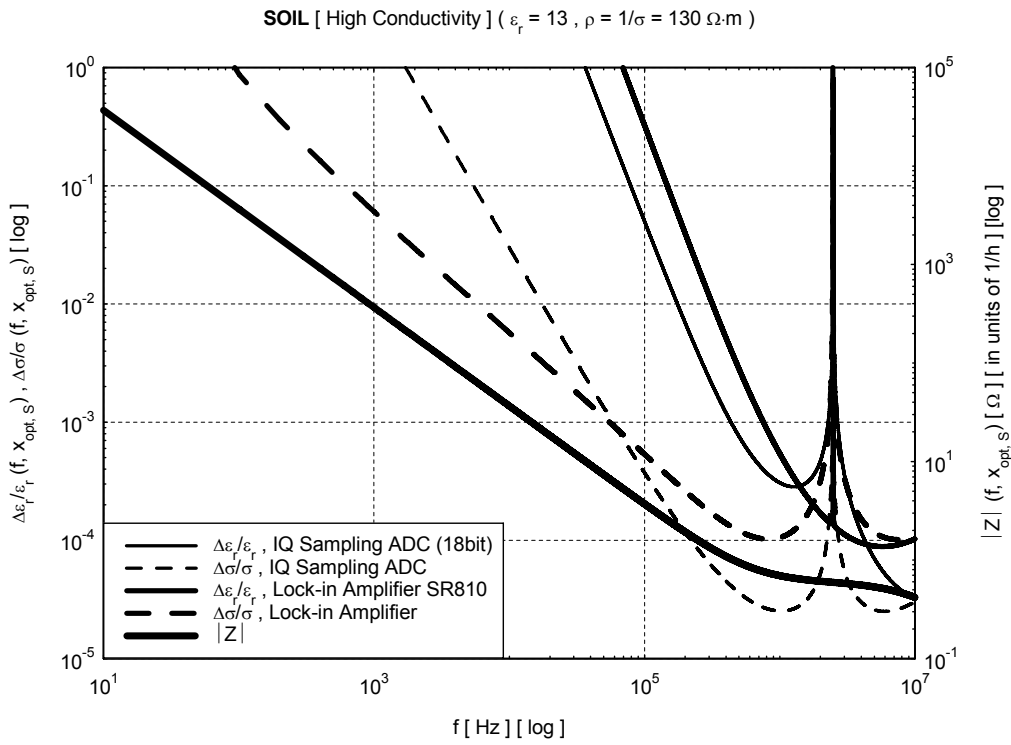


Figure 4.b

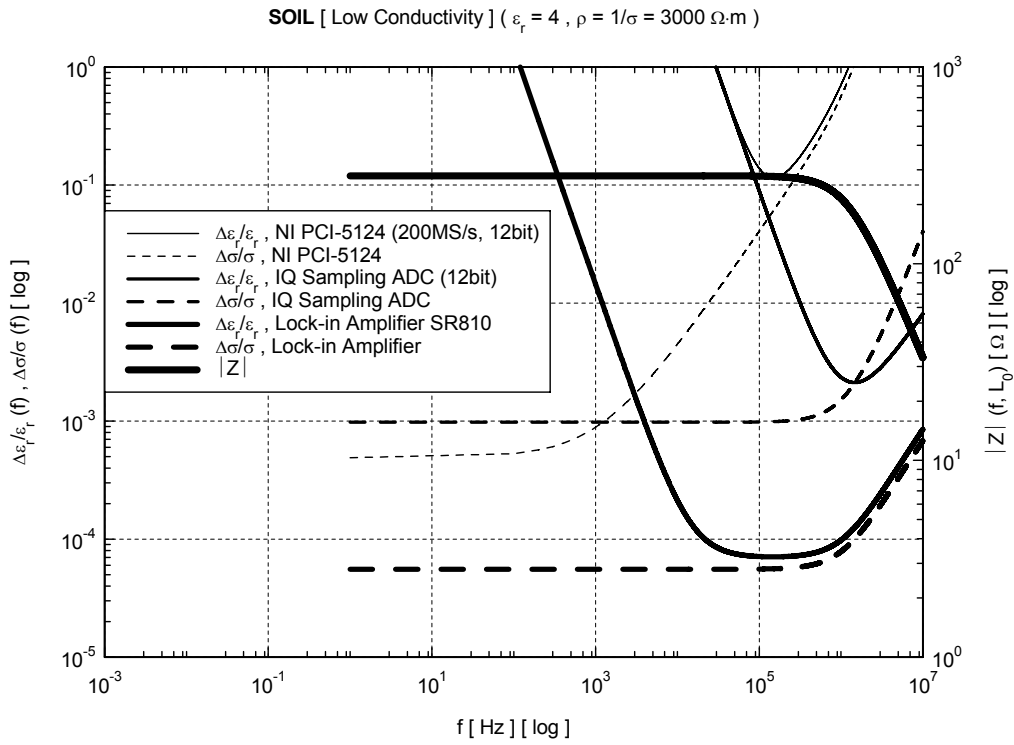


Figure 4.b.bis

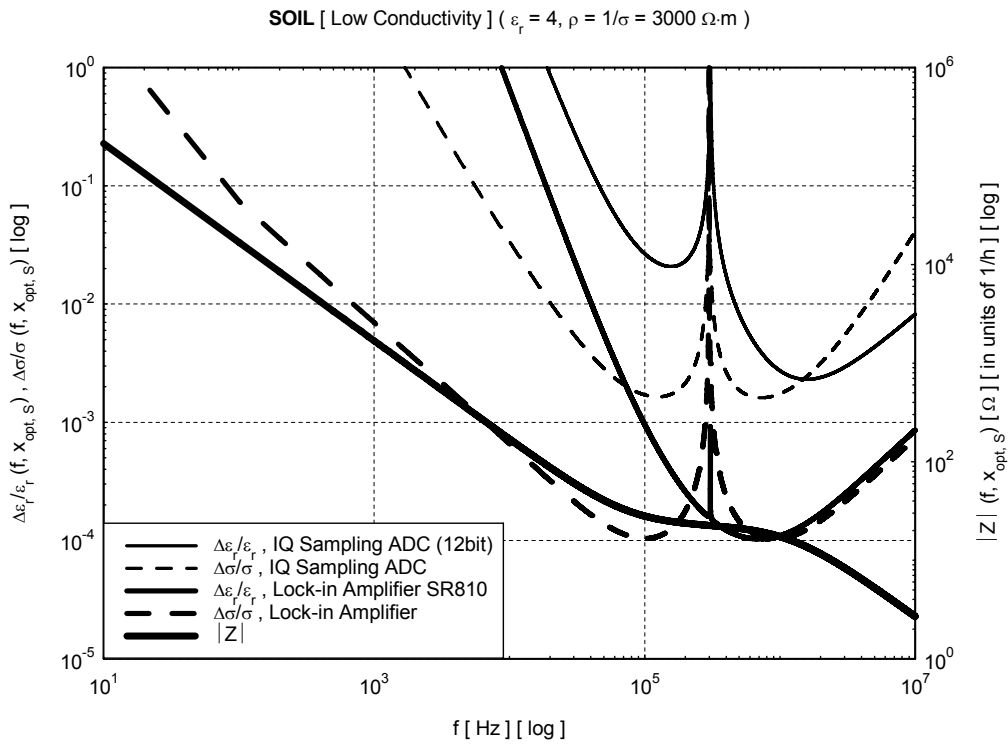


Figure 4.c

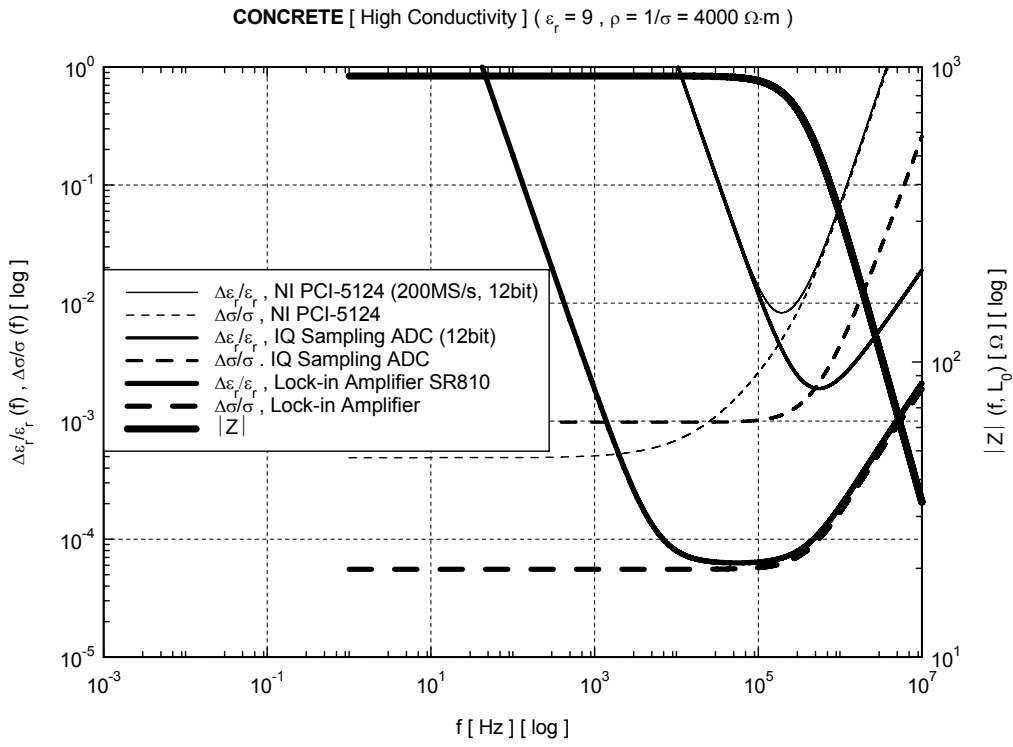


Figure 4.c.bis

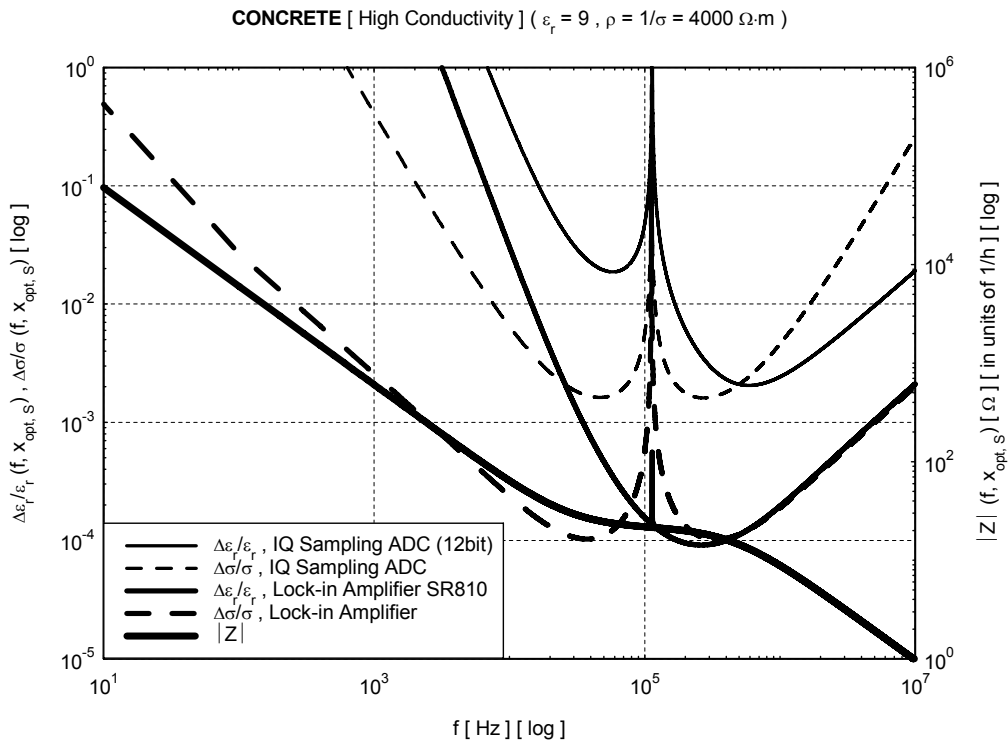


Figure 4.d

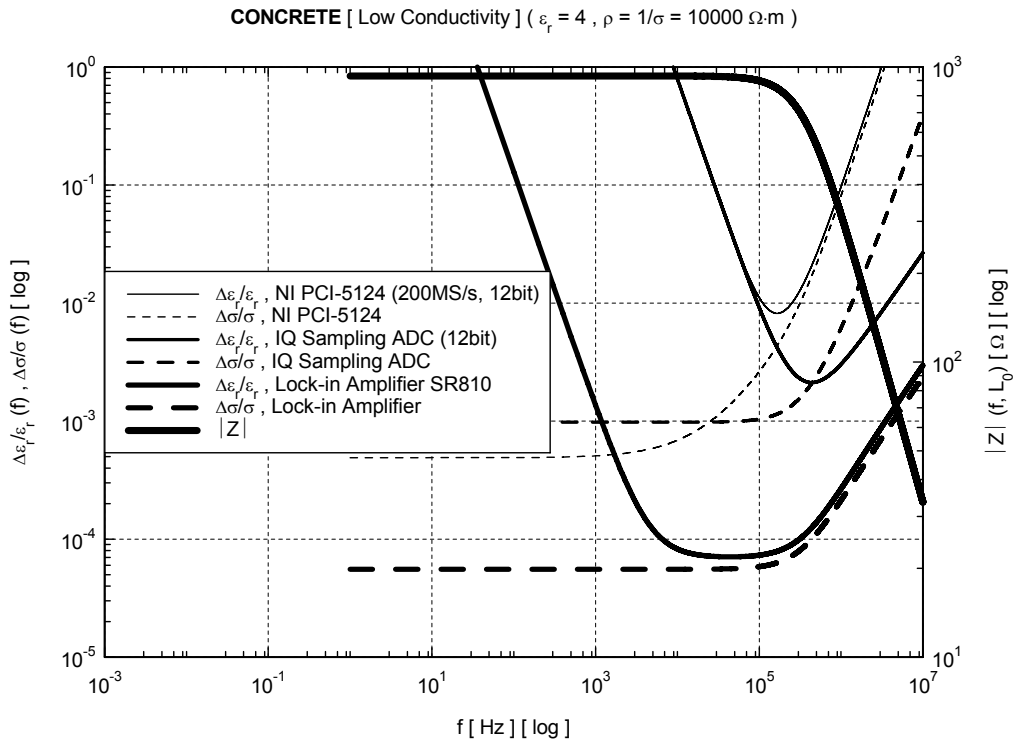


Figure 4.d.bis

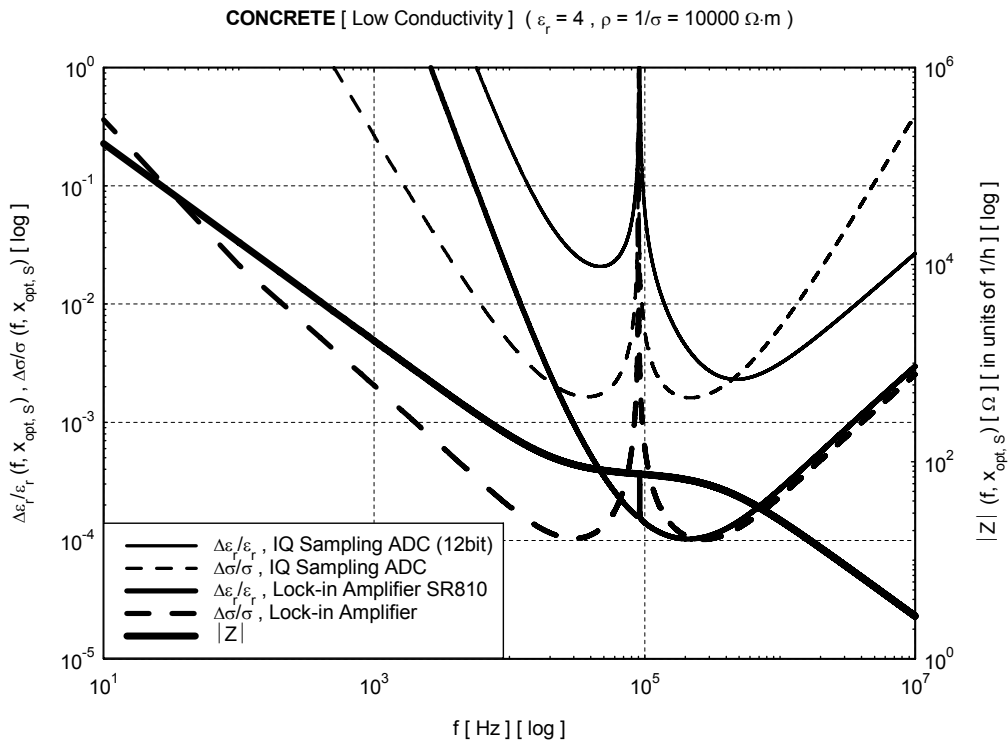


Figure 5.a

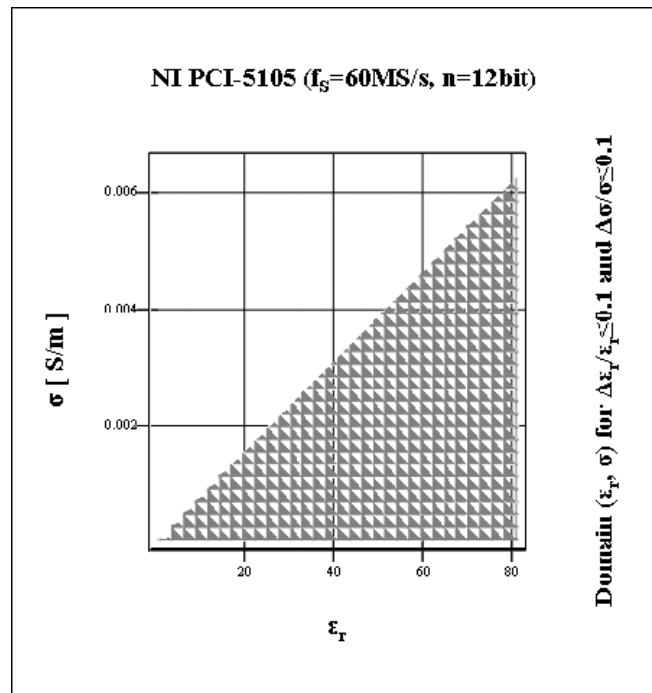


Figure 5.b

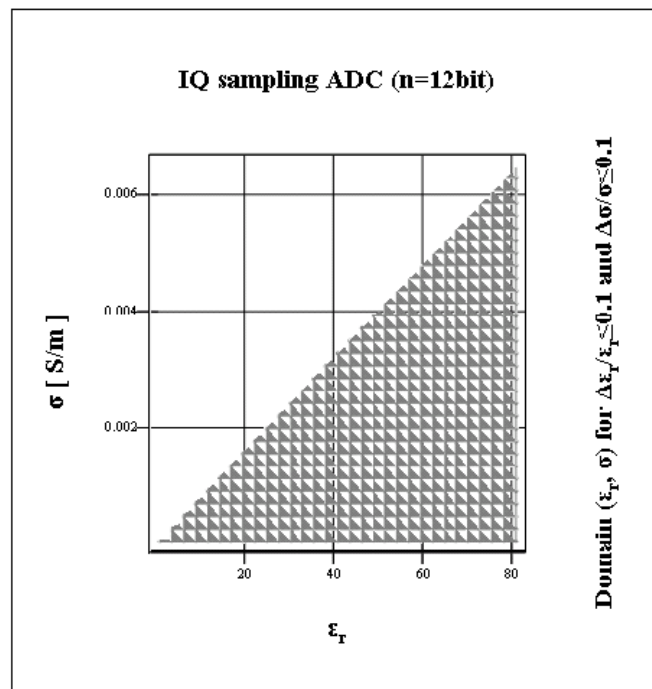


Figure 5.c

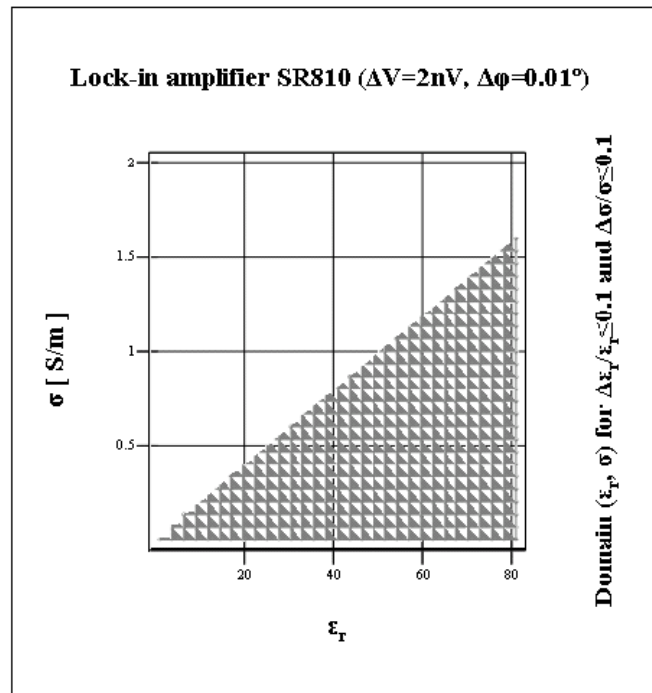


Figure 6.a

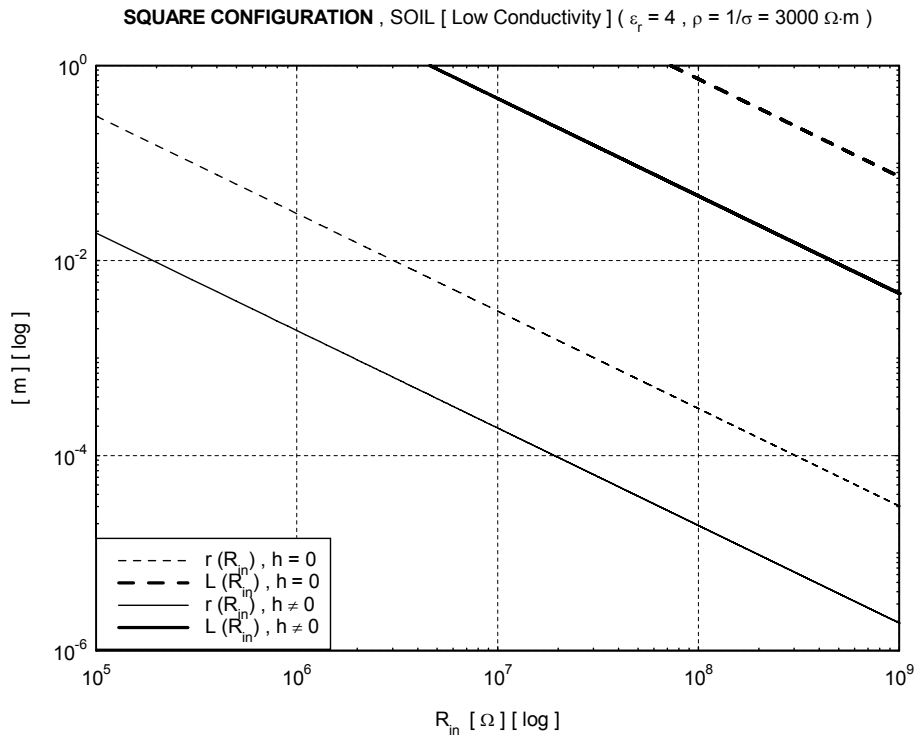


Figure 6.b

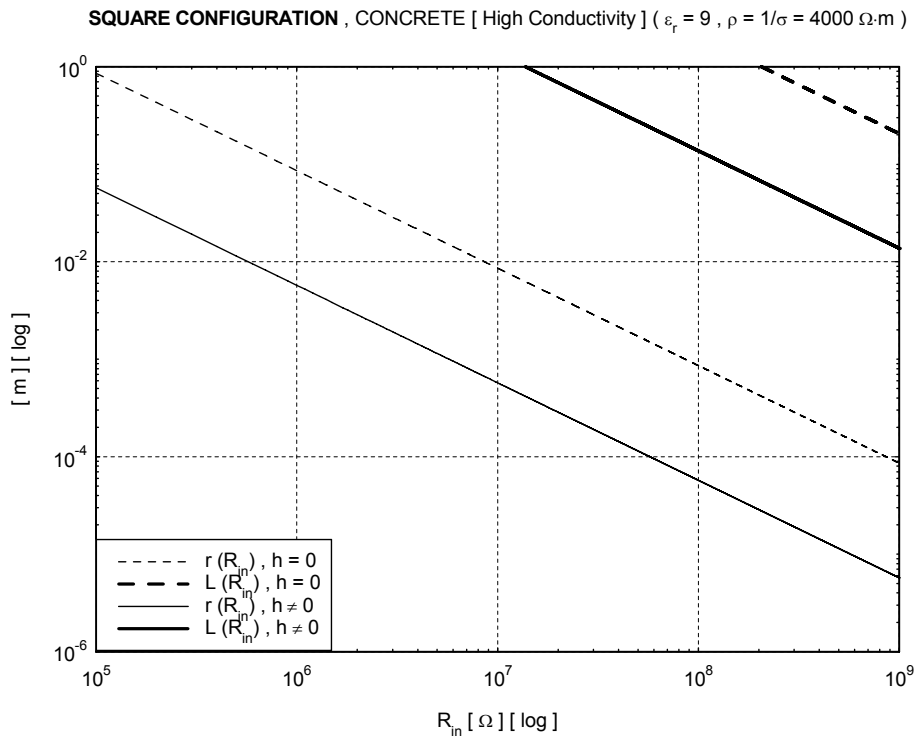


Figure 6.c

SQUARE CONFIGURATION , CONCRETE [Low Conductivity] ($\epsilon_r = 4$, $\rho = 1/\sigma = 10000 \Omega \cdot m$)

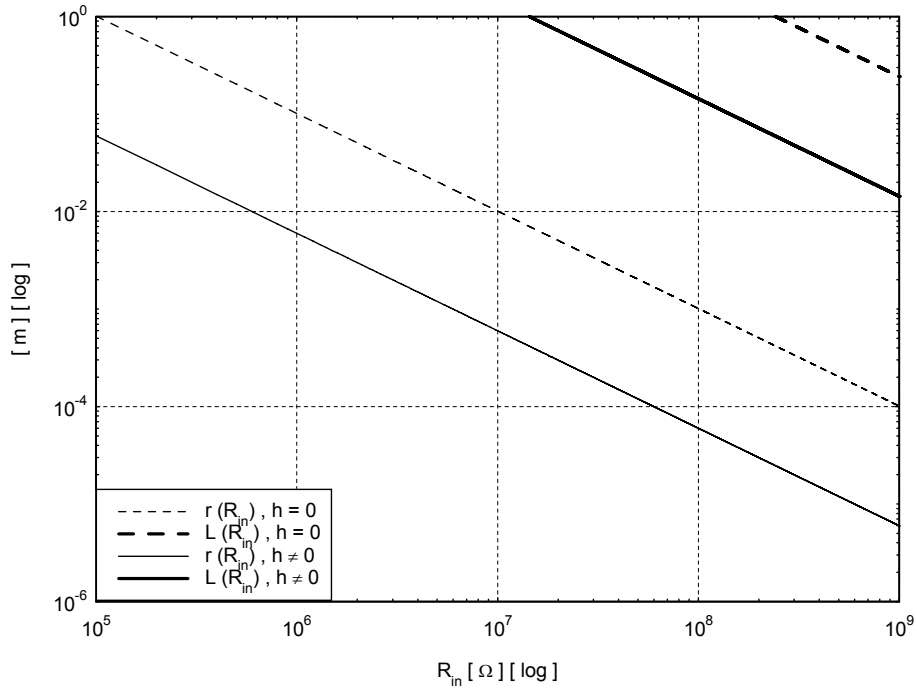


Figure 6.d

WENNER'S CONFIGURATION , SOIL [Low Conductivity] ($\epsilon_r = 4$, $\rho = 1/\sigma = 3000 \Omega \cdot m$)

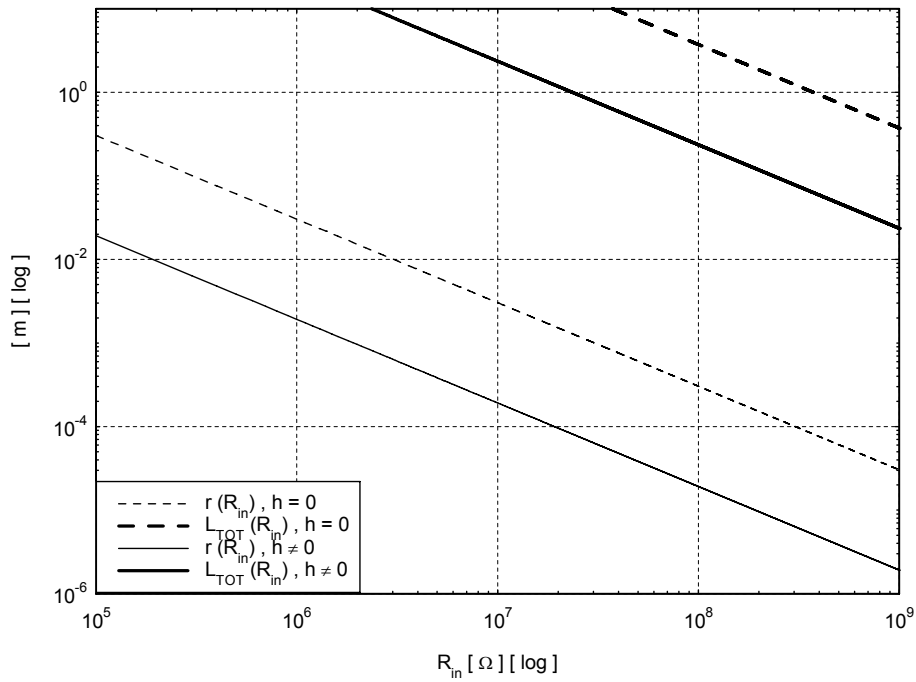


Figure 7.a

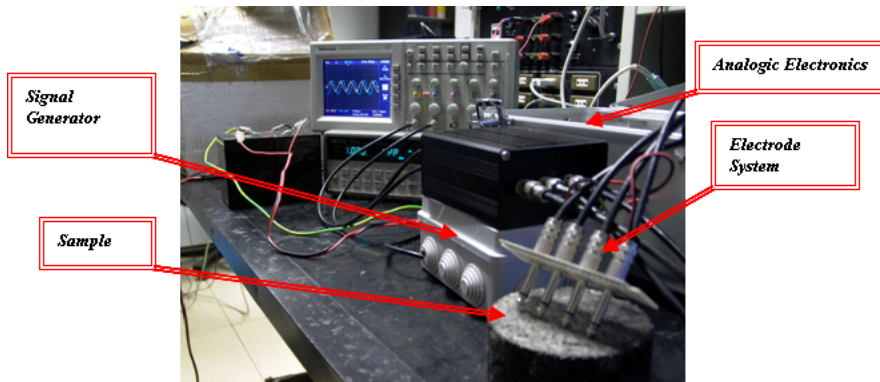


Figure 7.b

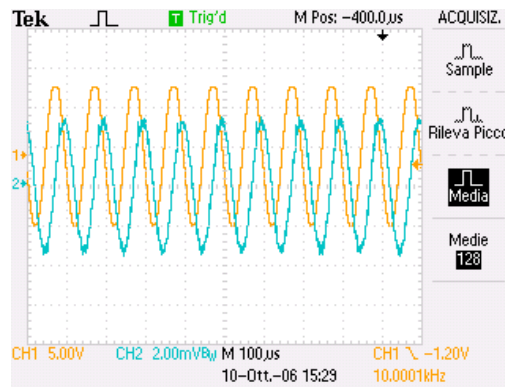


Table 1.a

$h = 0$ SOIL [High Conductivity] ($\epsilon_r = 13$, $\rho = 1/\sigma = 130 \Omega \cdot m$)	NI PCI-5922 ($f_s = 10 \text{ MS/s}$, $n = 18 \text{ bit}$)	IQ Sampling ADC ($n_{\min} = 18$)	Lock-in Amplifier SR810 ($\Delta V = 2 \text{ nV}$, $\Delta \phi = 0.01^\circ$)
f_{opt}	154.935 kHz	12.025 MHz	1.199 MHz
f_{min}	83.903 kHz	89.559 kHz	2.9 kHz
f_{max}	330.926 kHz	1.1236 GHz	10.333 GHz

Table 1.a.bis

$h \neq 0$ SOIL [High Conductivity] ($\epsilon_r = 13$, $\rho = 1/\sigma = 130 \Omega \cdot m$)	IQ Sampling ADC ($n_{\min} = 18$)	Lock-in Amplifier SR810 ($\Delta V = 2 \text{ nV}$, $\Delta \phi = 0.01^\circ$)
f_{up}	1.024 MHz	825.975 kHz
f_{low}	10.663 MHz	22.402 MHz

Table 1.b

$h = 0$ SOIL [Low Conductivity] ($\epsilon_r = 4$, $\rho = 1/\sigma = 3000 \Omega \cdot m$)	NI PCI-5124 ($f_s = 200 \text{ MS/s}$, $n = 12 \text{ bit}$)	IQ Sampling ADC ($n_{\min} = 12$)	Lock-in Amplifier SR810 ($\Delta V = 2 \text{ nV}$, $\Delta \phi = 0.01^\circ$)
f_{opt}	387.772 kHz	1.459 MHz	145.489 kHz
f_{min}	95.055 kHz	94.228 kHz	379.08 Hz
f_{max}	1.832 MHz	16.224 MHz	1.099 GHz

Table 1.b.bis

$h \neq 0$ SOIL [Low Conductivity] ($\epsilon_r = 4$, $\rho = 1/\sigma = 3000 \Omega \cdot m$)	IQ Sampling ADC ($n_{\min} = 12$)	Lock-in Amplifier SR810 ($\Delta V = 2 \text{ nV}$, $\Delta \phi = 0.01^\circ$)
f_{up}	124.768 kHz	100.508 kHz
f_{low}	1.492 MHz	780.277 kHz

Table 1.c

$h = 0$ CONCRETE [High Conductivity] ($\epsilon_r = 9$, $\rho = 1/\sigma = 4000 \Omega \cdot m$)	NI PCI-5124 ($f_s = 200 \text{ MS/s}$, $n = 12 \text{ bit}$)	IQ Sampling ADC ($n = 12$)	Lock-in Amplifier SR810 ($\Delta V = 2 \text{ nV}$, $\Delta \phi = 0.01^\circ$)
f_{opt}	193.94 kHz	547.144 kHz	54.558 kHz
f_{min}	33.315 kHz	33.292 kHz	134.02 Hz
f_{max}	1.206 MHz	6.084 MHz	463.74 MHz

Table 1.c.bis

$h \neq 0$ CONCRETE [High Conductivity] ($\epsilon_r = 9$, $\rho = 1/\sigma = 4000 \Omega \cdot m$)	IQ Sampling ADC ($n = 12$)	Lock-in Amplifier SR810 ($\Delta V = 2 \text{ nV}$, $\Delta \phi = 0.01^\circ$)
f_{up}	46.648 kHz	37.606 kHz
f_{low}	499.469 kHz	546.487 kHz

Table 1.d

$h = 0$ CONCRETE [Low Conductivity] ($\epsilon_r = 4$, $\rho = 1/\sigma = 10000 \Omega \cdot m$)	NI PCI-5124 ($f_s = 200 \text{ MS/s}$, $n = 12 \text{ bit}$)	IQ Sampling ADC ($n = 12$)	Lock-in Amplifier SR810 ($\Delta V = 2 \text{ nV}$, $\Delta \phi = 0.01^\circ$)
f_{opt}	165.329 kHz	437.637 kHz	43.647 kHz
f_{min}	28.273 kHz	28.268 kHz	113.724 Hz
f_{max}	1.016 MHz	4.867 MHz	329.796 MHz

Table 1.d.bis

$h \neq 0$ CONCRETE [Low Conductivity] ($\epsilon_r = 4$, $\rho = 1/\sigma = 10000 \Omega \cdot m$)	IQ Sampling ADC ($n = 12$)	Lock-in Amplifier SR810 ($\Delta V = 2 \text{ nV}$, $\Delta \phi = 0.01^\circ$)
f_{up}	37.43 kHz	30.152 kHz
f_{low}	477.58 kHz	234.083 kHz

Table 2.a

<i>SQUARE CONFIGURATION, SOIL [Low Conductivity] ($\epsilon_r = 4, \rho = 1/\sigma = 3000 \Omega \cdot m$)</i>	Galvanic Contact	Capacitive Contact
<i>L</i>	≈ 1 m	≈ 1 m
<i>R_{in}</i>	72.84 M Ω	4.6 M Ω
<i>r</i>	416.813 μ m	416.836 μ m

Table 2.b

<i>SQUARE CONFIGURATION, CONCRETE [High Conductivity] ($\epsilon_r = 9, \rho = 1/\sigma = 4000 \Omega \cdot m$)</i>	Galvanic Contact	Capacitive Contact
<i>L</i>	≈ 1 m	≈ 1 m
<i>R_{in}</i>	206.1 M Ω	13.74 M Ω
<i>r</i>	416.94 μ m	416.866 μ m

Table 2.c

<i>SQUARE CONFIGURATION, CONCRETE [Low Conductivity] ($\epsilon_r = 4, \rho = 1/\sigma = 10000 \Omega \cdot m$)</i>	Galvanic Contact	Capacitive Contact
<i>L</i>	≈ 1 m	≈ 1 m
<i>R_{in}</i>	242.8 M Ω	14.37 M Ω
<i>r</i>	416.819 μ m	416.858 μ m

Table 2.d

<i>WENNER'S LINEAR CONFIGURATION, SOIL [Low Conductivity] ($\epsilon_r = 4, \rho = 1/\sigma = 3000 \Omega \cdot m$)</i>	Galvanic Contact	Capacitive Contact
<i>L_{TOT} = 3·L</i>	≈ 10 m	≈ 10 m
<i>R_{in}</i>	37.3 M Ω	2.356 M Ω
<i>r</i>	813.959 μ m	813.856 μ m

Table 3

	Electrical Conductivity measured by the prototype	Dielectric Permittivity measured by the prototype
<i>Air</i>	9.1 10 ⁻⁸ S/m	1.28
<i>Coarse Grain Tar</i>	5.0 10 ⁻⁷ S/m	6.27
<i>Fine Grain Tar</i>	3.54 10 ⁻⁷ S/m	4.33
<i>Aggreagate Concrete</i>	2.4 10 ⁻⁶ S/m	7.05

Fig. 1. Equivalent circuit of the RESPER.

Fig. 1. Circuito equivalente del RESPER.

Fig. 2. Electrical scheme for the analogical part of the measuring system: a signal generator (1), coupled to an amplifier stage, feeds one of two current electrodes (T1). The same current signal, picked to the other electrode (T2), is converted into voltage (2) and then amplified (3). The stage of differentiation for the voltage (4) is preceded by the feedback device to compensate the parasite capacities (5). The signal is sent to an analogical digital converter (ADC) and transferred to a personal computer, where it can be properly processed. The electronic circuit is composed primarily from two stages. The first consists of a current-voltage converter followed by a cascade of amplifiers, to amplify the weak currents typical of high impedances and the second consists of a voltage amplifier with a retroactive chain of capacitive compensation. The circuit has been designed to work linearly at LF in the band from DC to 100kHz. The selected components have been developed specifically for electronic instruments of precision. The circuit techniques adopted for the compensation of the parasite capacities are innovative and allow to perform measurements of high impedances. This analogical device is connected to an analogical digital conversion board which contains even a digital analogical converter (DAC) used as a signal generator that, properly projected, can generate a whole series of measurements in an automatic way even at different frequencies for a full analysis.

Fig. 2. Schema elettrico per la parte analogica dello strumento: un generatore di segnale (1), accoppiato ad uno stadio di amplificazione, alimenta uno dei due elettrodi di corrente (T1). Lo stesso segnale di corrente, prelevato dall'altro elettrodo (T2), viene convertito in tensione (2) e poi amplificato (3). Lo stadio di differenziazione per la tensione (4) è preceduto dal dispositivo di controreazione per compensare le capacità parassite (5). Il segnale viene inviato ad un convertitore analogico digitale (ADC) e trasferito ad un *personal computer*, dove può essere opportunamente elaborato. Il circuito elettronico è composto principalmente da due stadi. Il primo è composto da un convertitore corrente tensione seguito da una cascata di amplificatori, per amplificare le deboli correnti caratteristiche di impedenze elevate e il secondo è composto da un amplificatore in tensione con una catena retroattiva di compensazione capacitiva. Il circuito è stato progettato per lavorare linearmente all'interno delle basse frequenze (LF) nella banda da DC a 100kHz. I componenti selezionati sono stati realizzati appositamente per la strumentazione elettronica di precisione. Le tecniche circuitali adottate per la compensazione delle capacità parassite sono innovative e permettono di realizzare misure di impedenze elevate. Questo dispositivo analogico è collegato ad una scheda di conversione analogico digitale che contiene anche un convertitore digitale analogico (DAC) utilizzato come generatore di segnali che, programmato adeguatamente, permette di generare tutta una serie di misure in modo automatico anche a diverse frequenze per una analisi completa.

Figs. 3. RESPER in square (a) or linear (Wenner's) (b) configuration.

Figs.3. RESPER in configurazione a quadrato (a) o lineare (di Wenner)(b).

Figs. 4. Bode's diagrams for the inaccuracies $\Delta\varepsilon_r/\varepsilon_r$ and $\Delta\sigma/\sigma$ in the measurement of the dielectric permittivity ε_r and the electrical conductivity σ , or for the modulus $|Z|$ of the transfer impedance, plotted as functions of the frequency f . The RESPER has a galvanic (height above ground $h=0$) (a-d) or capacitive (height/dimension ratio $x=x_{opt,S}$ optimally sized) (a.bis-d.bis) contact on non-saturated terrestrial soils characterized by an high ($\rho=1/\sigma=130\Omega\cdot m$, $\varepsilon_r=13$) (a, a.bis) and low ($\rho=3000\Omega\cdot m$, $\varepsilon_r=4$) (b, b.bis) conductivity or concretes with an high ($\rho=1/\sigma=4000\Omega\cdot m$, $\varepsilon_r=9$) (c, c.bis) and low ($\rho=10000\Omega\cdot m$, $\varepsilon_r=4$) (d, d.bis) conductivity. The quadrupolar probe is designed in the square configuration ($L_0=1m$) and is connected to a lock-in amplifier with specifications only similar to the SR810 and SR830's ones ($\Delta V=2nV$, $\Delta\varphi=0.01^\circ$), commercialized by the Standford Research Systems Company, or a uniform sampling ADC only similar to

the NI PCI-5922 ($f_s=10MS/s$, $n=18bit$) and NI PCI-5124 ($f_s=200MS/s$, $n=12bit$), commercialized by the National Instruments Company, or otherwise one of the IQ sampling ADCs with $n=18bit$ and $n=12bit$, which are being projected in our laboratories under the worst operative conditions, when an internal quartz is oscillating at its lowest merit factor $Q \approx 10^4$. The ADCs allow the lowest minimum value of frequency f_{min} , within the band $B=100kHz$, such that the inaccuracies in the measurements result below a prefixed limit, 15% referring to (a, a.bis) and 10% for (b-d, b.bis-d.bis) [Tabs. 1].

Figs. 4. Diagrammi di Bode per le incertezze $\Delta\varepsilon_r/\varepsilon_r$ and $\Delta\sigma/\sigma$ nelle misure della permittività dielettrica ε_r e conducibilità elettrica σ , o per il modulo $|Z|$ della impedenza di trasferimento, tracciate come funzioni della frequenza f . Il RESPER presenta un contatto galvanico (altezza da terra $h=0$) (a-d) o capacitivo (rapporto altezza/dimensione $x=x_{opt,S}$, calibrato ottimamente) (a.bis-d.bis) su suoli terrestri non-saturi caratterizzati da un alta ($\rho=1/\sigma=130\Omega\cdot m$, $\varepsilon_r=13$) (a, a.bis) e bassa ($\rho=3000\Omega\cdot m$, $\varepsilon_r=4$) (b, b.bis) conducibilità o calcestruzzi non saturi con un alta ($\rho=1/\sigma=4000\Omega\cdot m$, $\varepsilon_r=9$) (c, c.bis) e bassa ($\rho=10000\Omega\cdot m$, $\varepsilon_r=4$) (d, d.bis) conducibilità. La sonda a quadripolo è progettata nella configurazione a quadrato ($L_0=1m$) ed è connessa ad un amplificatore *lock-in* con specifiche solo simili a quelle dei SR810 e SR830 ($\Delta V=2nV$, $\Delta\varphi=0.01^\circ$), commercializzati dalla Standford Research Systems Company, o un ADC a campionamento uniforme solo simile ai NI PCI-5922 ($f_s=10MS/s$, $n=18bit$) e NI PCI-5124 ($f_s=200MS/s$, $n=12bit$), commercializzati dalla National Instruments Company, o altrimenti uno degli ADC a campionamento IQ con $n=18bit$ e $n=12bit$, che sono in fase di progettazione nei nostri laboratori in condizioni peggiorative, quando un quarzo interno oscilla al suo più basso fattore di merito $Q \approx 10^4$. L'ADC consente il più basso valore minimo di frequenza f_{min} , entro la banda $B=100kHz$, in modo tale che le incertezze nelle misure risultino al di sotto di un limite prefissato, il 15% con riferimento a (a, a.bis) e il 10% per (b-d, b.bis-d.bis) [Tab. 1].

Figs. 5. Plots for the domain (σ, ε_r) of the electrical conductivity σ and the dielectric permittivity ε_r such that both the inaccuracies $\Delta\sigma/\sigma(\sigma, \varepsilon_r)$, in the measurement of the conductivity σ , and $\Delta\varepsilon_r/\varepsilon_r(\sigma, \varepsilon_r)$, of the permittivity ε_r , result below a prefixed limit of 10%. The RESPER ($B=100kHz$) has a galvanic contact with the subjacent medium ($h=0$) and is connected to a low-cost uniform sampling ADC with specifications similar to the NI PCI-5105's one ($f_s=60MS/s$, $n=12bit$) (a), or an IQ sampling ADC, specified by $n=12bit$ (b), or otherwise a lock-in amplifier similar to the SR810 and SR830 ($\Delta V=2nV$, $\Delta\varphi=0.01^\circ$) (c).

Figs. 5. Grafici per il dominio (σ, ε_r) delle conducibilità elettrica σ e permittività dielettrica ε_r tale che sia le incertezze $\Delta\sigma/\sigma(\sigma, \varepsilon_r)$, nella misura della conducibilità σ , che $\Delta\varepsilon_r/\varepsilon_r(\sigma, \varepsilon_r)$, della permittività ε_r , risultino al di sotto di un limite prefissato del 10%. Il RESPER ($B=100kHz$) presenta un contatto galvanico con il mezzo sottostante ($h=0$) ed è connesso ad un ADC a campionamento uniforme e basso costo con specifiche simili a quelle del NI PCI-5105 ($f_s=60MS/s$, $n=12bit$) (a), o un ADC a campionamento IQ, specificato da $n=12bit$ (b), o altrimenti un amplificatore *lock-in* simile ai SR810 e SR830 ($\Delta V=2nV$, $\Delta\varphi=0.01^\circ$) (c).

Figs. 6. Like-Bode's diagrams of the minimal radius $r(R_{in}, f_{min})$ for the RESPER electrodes and of the characteristic geometrical dimension $L_S(r, n_{min})$ for the square configuration or the length $L_{TOT}(r, n_{min})=3 \cdot L_W(r, n_{min})$ for the (Wenner's) linear configurations, plotted as functions of the input resistance R_{in} for the amplifier stage. The quadropole probe could be designed for both galvanic and capacitive contact: the square configuration, on non-saturated terrestrial soils characterized by a low conductivity ($\rho=3000\Omega\cdot m$, $\varepsilon_r=4$) (a) or concretes with an high ($\rho=1/\sigma=4000\Omega\cdot m$, $\varepsilon_r=9$) (b) and low ($\rho=10000\Omega\cdot m$, $\varepsilon_r=4$) (c) conductivity; the Wenner's linear configuration, for galvanic and capacitive contact on terrestrial soils characterized by a low conductivity ($\rho=3000\Omega\cdot m$, $\varepsilon_r=4$) (d) [Tabs. 2]. The quadropole is connected to an IQ sampling ADC with minimal bit resolution $n_{min}=12$, which allows inaccuracies in the measurements below a prefixed limit (10%) within the LF band $[f_{min}, f_{max}]$ for operative conditions of galvanic contact or in the MF-HF band $[f_{up}, f_{low}]$ for capacitive contact [Tab. 1].

Figs. 6. Simil-diagrammi di Bode del raggio minimo $r(R_{in}, f_{min})$ per gli elettrodi del RESPER e della dimensione geometrica caratteristica $L_S(r, n_{min})$ per la configurazione a quadrato o della lunghezza $L_{TOT}(r, n_{min})=3 \cdot L_W(r, n_{min})$ per la configurazione lineare (o di Wenner), tracciati come funzioni della resistenza

di ingresso R_{in} per lo stadio amplificatore. La sonda a quadripolo potrebbe essere progettata sia per il contatto galvanico che capacitivo: la configurazione a quadrato, su suoli terrestri non saturi caratterizzati da una bassa conducibilità ($\rho=3000\Omega\cdot m$, $\varepsilon_r=4$) (a) o calcestruzzi non saturi con un elevata ($\rho=1/\sigma=4000\Omega\cdot m$, $\varepsilon_r=9$) (b) e bassa ($\rho=10000\Omega\cdot m$, $\varepsilon_r=4$) (c) conducibilità; la configurazione lineare di Wenner, per contatto galvanico e capacitivo su suoli terrestri caratterizzati da una bassa conducibilità ($\rho=3000\Omega\cdot m$, $\varepsilon_r=4$) (d) [Tabs. 2]. Il quadripolo è connesso ad un ADC a campionamento IQ con risoluzione minima di bit $n_{min}=12$, che permette incertezze nelle misure al di sotto di un limite prefissato (10%) all'interno della banda LF $[f_{min}, f_{max}]$ per le condizioni operative di contatto galvanico o nella banda MF-HF $[f_{up}, f_{low}]$ per contatto capacitivo [Tab. 1].

Fig. 7.a. The first prototype of a measuring system during the test on a block of tar. One can see the high-voltage signal generator (white box), the analogical electronics (black box), the prototype system of electrodes, put on a sample of tar, and the oscilloscope which digitizes the two signals, current and voltage, and displays them in the time domain. In the future developing, the electronics will be further integrated to render the system as compact as possible.

Fig. 7.a. Il primo prototipo dello strumento durante la fase di test su di un blocco di catrame. Sono visibili il generatore di alta tensione (scatola bianca), l'elettronica analogica (scatola nera) e il sistema di punte prototipale (poggiato su un campione di catrame) e l'oscilloscopio, che digitalizza i due segnali, di corrente e di tensione, e li visualizza nel dominio del tempo. Nello sviluppo successivo, l'elettronica verrà ulteriormente integrata per rendere lo strumento il più compatto possibile.

Fig. 7.b. The two signals, of voltage V (yellow line) and current V_I (in blue), acquired on the sample of tar in fig. 7.a: the two signals are almost out of phase ($\sim 90^\circ$), as expected for a predominantly capacitive transfer impedance.

Fig. 7.b I due segnali, di tensione V (in giallo) e corrente V_I (in blu), acquisiti sul campione di catrame in fig. 7.a: i due segnali sono quasi sfasati di ($\sim 90^\circ$), come ci si aspetta per un'impedenza di trasferimento prevalentemente capacitiva.

Tab. 3. First results of laboratory tests, performed on samples of different materials. The values are compatible with those in literature. These initial steps have enabled to evaluate the validity of the instrumentation and the correctness of the used method. The device is shown stable varying the peak-peak amplitude of the signal for a frequency range which extends from few kHz to around $100kHz$.

Tab. 3. I primi risultati degli esami di laboratorio, effettuati su campioni di materiali diversi. I valori sono compatibili con quelli in letteratura. Questi passi iniziali hanno consentito di valutare la validità della strumentazione e la correttezza del metodo utilizzato. Il dispositivo si è dimostrato stabile, variando l'ampiezza di picco-picco del segnale per una banda di frequenze che si estende da pochi kHz a circa $100kHz$.